

Sifting through the Noise: A Survey of Diffusion Probabilistic Models and Their Applications to Biomolecules

Trevor Norton¹ and Debswapna Bhattacharya*¹

¹Department of Computer Science, Virginia Tech, Blacksburg, Virginia, 24061, USA

Abstract

Diffusion probabilistic models have made their way into a number of high-profile applications since their inception. In particular, there has been a wave of research into using diffusion models in the prediction and design of biomolecular structures and sequences. Their growing ubiquity makes it imperative for researchers in these fields to understand them. This paper serves as a general overview for the theory behind these models and the current state of research. We first introduce diffusion models and discuss common motifs used when applying them to biomolecules. We then present the significant outcomes achieved through the application of these models in generative and predictive tasks. This survey aims to provide readers with a comprehensive understanding of the increasingly critical role of diffusion models.

1 Introduction

Diffusion probabilistic models (or more simply diffusion models) have attracted attentions from researchers and the public alike for their success in image generation. After usurping generative adversarial networks (GANs) in sampling high-quality images [1, 2], we have seen many diffusion-based image synthesis models introduced. Diffusion models have also been successfully applied to problems in computer vision [3], audio generation [4, 5, 6], robotics [7, 8, 9, 10, 11], and many others.

Diffusion models are a category of deep generative models, which seek to easily sample some underlying distribution $p(x)$. Sampling a distribution can be difficult in cases where the distribution has many modes or is in a high-dimensional space. This problem can be especially prevalent when working with thermodynamic systems, where energy barriers can prevent adequate exploration of the distribution. Non-machine learning techniques have relied on expensive search methods, such as Markov chain Monte Carlo (MCMC) simulations, to accurately sample a distribution [12, 13, 14, 15]. Diffusion models instead sample a tractable prior (a normal distribution, for example), which is then transformed into the correct distribution. They do this by adding Gaussian noise to the data distribution and then learning how to iteratively remove the noise. This iterative denoising breaks down the generation process into simpler, learnable steps and allows sampling from very high-dimensional, rough distributions.

This ability makes diffusion models an attractive choice for the modeling of biomolecules. Problems in the field typically result in very high-dimensional data that have rough distributions. Levinthal’s paradox [16] famously noted this difficulty with the protein folding problem: put simply, if one were to search every possible conformation of a protein for its native structure, it would take longer than the age of the universe (even if checking the state only took on the order of picoseconds). The outlook worsens when one considers that the energy landscape may have several meta-stable states that are not the native structure. Because of this, straight-forward calculations are usually intractable, and deep learning methods have provided tremendous leaps forward in predictive tasks. Most saliently, AlphaFold2 has been able to provide experimental accuracy of the native folded structures for many proteins [17]. Diffusion models benefit from scalable deep learning architectures and can circumvent the issues of dimensionality through the iterative process. Furthermore,

*Correspondence to dbhattacharya@vt.edu

the diffusion process progressively smooths out the underlying distribution, which makes the new, smoother distributions amenable to approximation via deep neural networks [18].

Research into applications of diffusion models to biomolecules has exploded in recent years, and there have already been a series of successes. This paper seeks to give an overview of the current state of diffusion models in the field and highlight the strengths and weaknesses of the method. We will first proceed by giving a brief history of diffusion models and their derivations. Following this, we details some of the most common techniques used when directly applying diffusion models to problems involving biomolecules. The remainder of the paper summarizes recent results and looks at possible future areas of research.



Figure 1: Illustration of a diffusion process in three dimensions. A molecule, such as a protein or RNA, can be represented by a collection of points in Euclidean space. The diffusion process gradually adds noise until the distribution is approximately normal. A diffusion model learns to denoise, so that samples from a normal distribution can be converted back to samples of the original distribution.

2 Preliminaries on diffusion models

Early diffusion models were heavily inspired by techniques from thermodynamics and statistics. The common observation among them was that it is possible to progressively transform a normal distribution into a given data distribution. However, the theories behind this transformation differed. Some viewed this process as learning to reverse a noising process, where the model progressively removes noise from a sample. Others thought about this process as accurately sampling a continuous family of perturbed distributions. Both theories can be unified into a flexible framework where the diffusion is described by continuous processes. In this section, we briefly recall the early work on diffusion models and the main results.

2.1 Denoising diffusion probabilistic modeling

Inspired by techniques in nonequilibrium thermodynamics and statistics [19, 20], Sohl-Dickstein et al. first proposed diffusion models as a way to develop probabilistic models that are flexible enough to capture complex distributions while providing exact sampling [21]. The main idea behind the algorithm was to start with samples from the desired distribution and iterative inject Gaussian noise until approximately reaching a stationary standard normal distribution. Training the model then comes down to learning how to reverse the noising process and recover the initial distribution.

More concretely, we want to approximate the distribution of data given as $\mathbf{x}_0 \sim p_{\text{data}}(\mathbf{x}_0)$. The forward process is a Markov chain whose transitions are given by Gaussian distributions according to a variance schedule $0 < \beta_1, \dots, \beta_T < 1$:

$$q(\mathbf{x}_t | \mathbf{x}_{t-1}) := \mathcal{N}(\mathbf{x}_t; \sqrt{1 - \beta_t}\mathbf{x}_{t-1}, \beta_t\mathbf{I}).$$

The transition kernel can be given exactly as

$$q(\mathbf{x}_t | \mathbf{x}_0) = \mathcal{N}(\mathbf{x}_t; \sqrt{\alpha_t}\mathbf{x}_0, (1 - \alpha_t)\mathbf{I}),$$

where $\alpha_t = \prod_{i=1}^t (1 - \beta_i)$, and so the exact distribution at time t is

$$q(\mathbf{x}_t) = \int q(\mathbf{x}_t | \mathbf{x}_0)p_{\text{data}}(\mathbf{x}_0) d\mathbf{x}_0.$$

After sufficiently many steps through the Markov chain, we have that $q(\mathbf{x}_T)$ is approximately equal to $\mathcal{N}(\mathbf{x}_T | \mathbf{0}, \mathbf{I})$, the stationary distribution of the process.

To recover p_{data} , we want to parameterize a reverse Markov chain p_θ that will take the distribution $\mathcal{N}(\mathbf{0}, \mathbf{I})$ and iteratively remove the added Gaussian noise. If the size of the steps β_t are small enough, the reverse process can be approximated by Gaussian transitions [21] and so the reverse process is parameterized as

$$p_\theta(\mathbf{x}_{t-1} | \mathbf{x}_t) := \mathcal{N}(\mathbf{x}_{t-1}; \boldsymbol{\mu}_\theta(\mathbf{x}_t, t), \boldsymbol{\Sigma}_\theta(\mathbf{x}_t, t)).$$

Training in [21] is then based on maximizing an evidence lower bound (ELBO).

In [22], this model is updated to have a simplified variational bound which improves sample quality. Reparameterizing the reverse process by setting

$$\boldsymbol{\mu}_\theta(\mathbf{x}_t, t) = \frac{1}{\sqrt{1 - \beta_t}} \left(\mathbf{x}_t - \frac{\beta_t}{\sqrt{1 - \alpha_t}} \boldsymbol{\epsilon}_\theta(\mathbf{x}_t, t) \right)$$

and rescaling the loss gives a simplified training objective

$$L_{\text{DDPM}}(\theta) := \mathbb{E}_{t, \mathbf{x}_0, \boldsymbol{\epsilon}} [\|\boldsymbol{\epsilon} - \boldsymbol{\epsilon}_\theta(\sqrt{\alpha_t} \mathbf{x}_0 + \sqrt{1 - \alpha_t} \boldsymbol{\epsilon}, t)\|^2],$$

where $\boldsymbol{\epsilon} \sim \mathcal{N}(\mathbf{0}, \mathbf{I})$. This diffusion model with L_{DDPM} is known as a Denoising Diffusion Probabilistic Model (DDPM).

2.2 Noise conditional score network

In [23], the authors approach the problem of sampling from an unknown distribution p_{data} by estimating its (Stein) score $\nabla_{\mathbf{x}} \log p_{\text{data}}(\mathbf{x})$ at varying noise levels. The score is related to ideas from statistical mechanics. Namely, if we have an energy function $E(\mathbf{x})$, then the associated Boltzmann distribution of the data is given according to

$$p(\mathbf{x}) = \frac{\exp(-E(\mathbf{x}))}{Z},$$

where Z is a normalizing factor that is typically intractable to compute. Thus determining the score of the distribution is essentially equivalent to finding $-\nabla E(\mathbf{x})$, from which Langevin dynamics of the system may be computed.

Theoretically, approximating $\nabla_{\mathbf{x}} \log p_{\text{data}}$ would allow sampling of the distribution directly through simulations. However, as Song et al. note, there are two major challenges with this approach:

- (1) Typically data lies on a low-dimensional manifold in the ambient space, in which case the score may be undefined or difficult to accurately approximate.
- (2) There may be low-density regions of the distribution. This results in poor initial sampling of the distribution in those spaces making it harder to estimate the score. Furthermore, when sampling with Langevin dynamics, slow mixing can occur leading to inaccurate estimates of the distribution in the short term.

Both challenges can be addressed by instead estimating the scores of perturbations of p_{data} . The perturbation kernel is defined as

$$q_\sigma(\mathbf{x} | \mathbf{x}') := \mathcal{N}(\mathbf{x}; \mathbf{x}', \sigma^2 \mathbf{I}),$$

so that the data distribution is perturbed to

$$q_\sigma(\mathbf{x}) = \int q(\mathbf{x} | \mathbf{x}') p_{\text{data}}(\mathbf{x}') d\mathbf{x}'.$$

The aim of the model is to approximate the score $\nabla_{\mathbf{x}} \log q_\sigma(\mathbf{x})$ for increasing levels of noise $\sigma_{\min} = \sigma_1 < \sigma_2 < \dots < \sigma_N = \sigma_{\max}$. The levels of noise are chosen so that $q_{\sigma_{\min}}(\mathbf{x}) \approx p_{\text{data}}(\mathbf{x})$ and $q_{\sigma_{\max}}(\mathbf{x}) \approx \mathcal{N}(\mathbf{x}; \mathbf{0}, \mathbf{I})$. Thus there will be a family of distributions ending with pure noise and progressively getting closer to the desired distribution.

A *noise conditional score network* (NCSN) $s_\theta(\mathbf{x}, \sigma)$ is trained to estimate the scores at the specified noise levels. There are several techniques to approximate the scores, but most implementations use *denoising score matching* which seeks to minimize

$$\mathbb{E}_{q_\sigma(\mathbf{x}|\mathbf{x}')p_{\text{data}}(\mathbf{x}')} [\|s_\theta(\mathbf{x}, \sigma) - \nabla_{\mathbf{x}} \log q_\sigma(\mathbf{x}|\mathbf{x}')\|^2].$$

Since the perturbation kernel is Gaussian, the gradient can be written exactly. Song et al. use the training objective

$$L_{\text{NCSN}}(\theta) := \sum_{i=1}^N \sigma_i^2 \mathbb{E}_{p_{\text{data}}(\mathbf{x}')} \mathbb{E}_{q_{\sigma_i}(\mathbf{x}|\mathbf{x}')} \left[\left\| s_\theta(\mathbf{x}, \sigma_i) + \frac{\mathbf{x} - \mathbf{x}'}{\sigma_i^2} \right\|^2 \right]$$

After training and determining $\theta^* = \operatorname{argmin}_\theta L_{\text{NCSN}}(\theta)$, sampling from the distribution is done by a series of Langevin simulations at each noise level. That is, M steps of the (overdamped) Langevin dynamics are performed for each σ_i :

$$\mathbf{x}_i^m = \mathbf{x}_i^{m-1} + \varepsilon_i s_{\theta^*}(\mathbf{x}_i^{m-1}, \sigma_i) + \sqrt{2\varepsilon_i} \mathbf{z}_i^m, \quad m = 1, 2, \dots, M$$

where $\varepsilon_i > 0$ is the step size and \mathbf{z}_i^m is standard normal. Then the final sample at the noise level \mathbf{x}_i^M is approximately distributed as $q_{\sigma_i}(\mathbf{x})$. The sampling is initialized with $\mathbf{x}_N^0 \sim \mathcal{N}(\mathbf{x} | \mathbf{0}, \sigma_{\max}^2 \mathbf{I})$. And each noise level is initialized with the terminal value of the previous noise level: $\mathbf{x}_i^0 = \mathbf{x}_{i+1}^M$. The final value, \mathbf{x}_1^M is an approximate sample from $p_{\text{data}}(\mathbf{x})$.

2.3 Score based modeling with stochastic differential equations

Previous diffusion models used discrete Gaussian noising process to transform their distributions into standard normal distributions. However, modeling the noising process as a stochastic differential equation (SDE), as suggested in [24], has many advantages. In particular, the framework is flexible and generalizes DDPMs and NCSNs as discretizations of different equations.

The forward diffusion process is modeled with an Itô SDE:

$$d\mathbf{x} = \mathbf{f}(\mathbf{x}, t)dt + g(t)d\mathbf{w}, \quad (1)$$

where \mathbf{w} is a standard Wiener process, $\mathbf{f} : \mathbb{R}^d \times [0, \infty) \rightarrow \mathbb{R}^d$ is the *drift* coefficient and $g : [0, \infty) \rightarrow \mathbb{R}$ is the *diffusion* coefficient. The initial condition \mathbf{x}_0 has the distribution of the data, $p_0(\mathbf{x})$, and it is assumed that for a sufficiently long time T that \mathbf{x}_T is approximately distributed as the stationary solution of eq. (1).

Taking the step sizes for DDPMs and NCSNs to zero gives a continuous version of the models that we can write as SDEs. The DDPM converges to the SDE

$$d\mathbf{x} = -\frac{1}{2}\beta(t)\mathbf{x}dt + \sqrt{\beta(t)}d\mathbf{w},$$

which we refer to as the variance preserving (VP) SDE. Also, NCSNs converge to the SDE

$$d\mathbf{x} = \sqrt{\frac{d[\sigma(t)^2]}{dt}}d\mathbf{w},$$

which we refer to as the variance exploding (VE) SDE.

If the score $\nabla_{\mathbf{x}} \log p_t(\mathbf{x})$ is known, then the diffusion process can be reversed by the following SDE:

$$d\mathbf{x} = [\mathbf{f}(\mathbf{x}, t) - g(t)^2 \nabla_{\mathbf{x}} \log p_t(\mathbf{x})] dt + g(t)d\bar{\mathbf{w}}, \quad (2)$$

where $\bar{\mathbf{w}}$ is a standard Wiener process when time flows backward from T to 0. Thus the goal is to train a score network $s_\theta(\mathbf{x}, t)$ to approximate $\nabla_{\mathbf{x}} \log p_t(\mathbf{x})$. A typical objective for training is by again using denoising score matching:

$$\mathbb{E}_t \left\{ \lambda(t) \mathbb{E}_{p_0(\mathbf{x}')} \mathbb{E}_{p_{0,t}(\mathbf{x}|\mathbf{x}')} [\|s_\theta(\mathbf{x}, t) - \nabla_{\mathbf{x}} \log p_{0,t}(\mathbf{x} | \mathbf{x}')\|^2] \right\}.$$

Other score-matching objectives can also be used here, such as sliced score matching [25].

Apart from eq. (2), there is another method for reversing the diffusion process. The ODE

$$d\mathbf{x} = \left[\mathbf{f}(\mathbf{x}, t) - \frac{1}{2}g(t)^2 \nabla_{\mathbf{x}} \log p_t(\mathbf{x}) \right] dt \quad (3)$$

shares the same marginal probability densities as the SDE. One benefit of eq. (3) is that sampling can be done much quicker using standard ODE solvers versus the Euler–Maruyama method for integrating eq. (2). Furthermore, integrating the ODE provides identifiable latent representations of the data and exact likelihood computations.

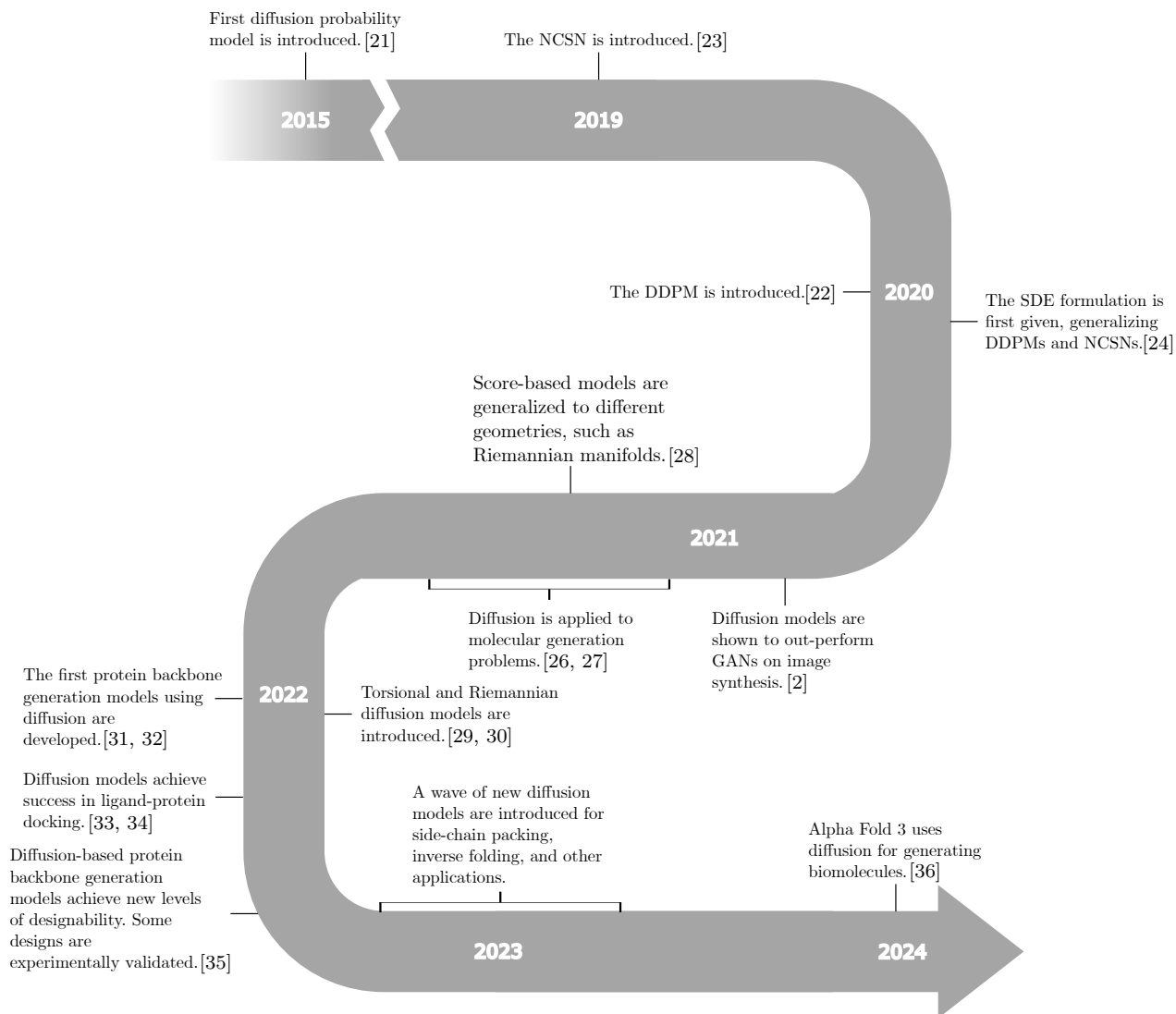


Figure 2: Timeline of applications of diffusion models to biomolecules.

3 Motifs for diffusion applied to biomolecules

Due to the geometry of biomolecules and the common goals of researchers, when diffusion is applied to problems in the field several techniques and ideas come up often. Some of these are standard notions for diffusion generally, but others are more niche. This section covers ideas that appear frequently in research with the aim of highlighting the most important concepts when engaging in the literature.

3.1 Controllable generation

Unconditionally sampling from the learned distribution of a diffusion model is usually insufficient for applications. For example, in protein design, one may desire not just a protein sequence and conformation but also that the final structure satisfies some prescribed function. The SDE formulation of diffusion models allows for a straight-forward description of controllable generation. Given an observation \mathbf{y} , the goal is to sample from the distribution of $\mathbf{x}(0)$ conditioned on \mathbf{y} , i.e., the distribution $p_0(\mathbf{x}(0) | \mathbf{y})$. The score of this distribution when perturbed can be rewritten using Bayes’ rule to get

$$\nabla_{\mathbf{x}} \log p_t(\mathbf{x}(t) | \mathbf{y}) = \nabla_{\mathbf{x}} \log p_t(\mathbf{x}(t)) + \nabla_{\mathbf{x}} \log p(\mathbf{y} | \mathbf{x}(t)).$$

Typically, $\nabla_{\mathbf{x}} \log p_t(\mathbf{x}(t))$ will be approximated by a score network and so $\nabla_{\mathbf{x}} \log p(\mathbf{y} | \mathbf{x}(t))$ will need to be estimated.

One option is to train another network to approximate this term. Training of the networks can often be done simultaneously so that the conditioned and unconditioned scores can be learned together. In some cases, domain knowledge or heuristics can be used to get an approximation. In the particular case of in-painting, the *replacement method* has been used to approximate the conditional gradient. However, as pointed out in [32], this leads to an irreducible error, but a similar method using particle filtering can guarantee an approximation with the correct limiting distribution.

3.2 Equivariant/Invariant score networks

For many problems involving biomolecules, the space is three-dimensional Euclidean space (that is, \mathbb{R}^3) and the results should not depend on the choice of coordinate axes. For example, when predicting the native structure of a protein, two conformations are equivalent if one can be transformed into the other by translations and rotations. To be precise, the solution should be *equivariant* (or *invariant*) to rigid motions. A function $f : \mathcal{X} \rightarrow \mathcal{Y}$ is equivariant with respect to a group G if for each $g \in G$ and $x \in \mathcal{X}$

$$f(g \cdot x) = g \cdot f(x),$$

where $g \cdot x$ and $g \cdot f(x)$ represents a group action on \mathcal{X} and \mathcal{Y} , respectively. A function is invariant if $f(g \cdot x) = f(x)$ for each $g \in G$ and $x \in \mathcal{X}$. Restricting machine learning architectures to the smaller space of equivariant functions speeds up training and makes models robust to such transformations. Thus, networks that are equivariant with respect to the special Euclidean group SE(3) are a natural choice for problems involving biomolecules¹.

A common choice for incorporating equivariance into diffusion models is to use an equivariant network for $s_\theta(\mathbf{x}, t)$. Given that the diffusion process and the score are both equivariant with respect to SE(3), the reverse diffusion and sampling processes are also equivariant (c.f. [26, Prop. 1] for instance). Common choices of architecture for the score network include Invariant Point Attention [17], Tensor Field Networks [37], and Equivariant Graph Neural Networks [38], among other.

3.3 Diffusion on manifolds

While equivariance provides numerous benefits when designing diffusion models, it may also lead unrealistic generation of molecules. This is due to the chirality of some biomolecules, which is not preserved under reflections of \mathbb{R}^3 . Furthermore, for molecules with n particles, the effective number of degrees of freedom is typically much smaller than $3n$. For instance, bond lengths and angles are usually fairly rigid in molecules and thus contribute little to the diversity of conformations. Thus, one can imagine the configurations of a biomolecule as lying on a smaller submanifold of the ambient space, and by defining coordinates on that manifold the configuration of the molecules can be specified. It is possible to define the diffusion process on these new coordinates, which reduces the dimension of the problem while enforcing certain geometric priors.

Score-based diffusion models may be carried over to Riemannian manifolds while retaining many of the characteristics of the models from Cartesian space [28]. A natural choice for forward diffusion on compact

¹Due to the chirality of certain biomolecules, one typically does not want equivariance to *reflections*. Hence, equivariance/invariance is typically with respect to SE(3) and not E(3)

manifolds is the VE SDE

$$d\mathbf{x} = \sqrt{\frac{d[\sigma(t)^2]}{dt}} d\mathbf{w}_{\mathcal{M}},$$

where $\mathbf{w}_{\mathcal{M}}$ is now Brownian motion on the manifold. This SDE has a uniform distribution as its stationary distribution. For generic Riemannian manifolds, the transition kernel cannot be explicitly written, and so training may be computationally expensive. However, the kernel is known for some simple manifolds. For rigid bodies in three dimensions, two manifolds are particularly useful: the torus \mathbb{T} , and the set of orientations $\text{SO}(3)$.

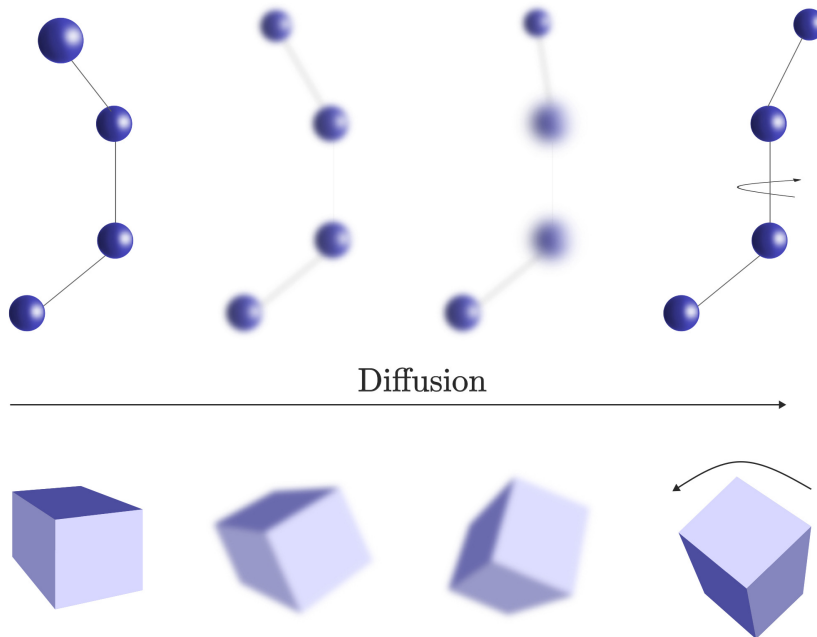


Figure 3: Sample paths for diffusion in \mathbb{T} and $\text{SO}(3)$. (top) Diffusion in \mathbb{T} is frequently applied to the torsion angle of four consecutive particles. Since bond lengths and angles are usually fairly rigid, most of the diversity in conformations can be explained by the torsional angles. Here an example torsional angle is perturbed by the diffusion process. (bottom) Diffusion in $\text{SO}(3)$ can be applied to frame data to perturb the orientation. Here the cube’s center is not moved while a rigid rotation is applied.

3.3.1 Diffusion on \mathbb{T} : torsional space

The manifold \mathbb{T} can be used to represent angular data, with the points being associated with the interval $[0, 2\pi)$ [29]. The conformation for many molecules can almost entirely be described by their torsional angles, and so modeling the diffusion process on \mathbb{T}^m can effectively reduce the dimensionality without a significant loss of accuracy.

For the VE formulation the transition kernel on \mathbb{T}^m is given by the wrapped Gaussian:

$$p_t(\boldsymbol{\tau} | \boldsymbol{\tau}') \propto \sum_{\mathbf{k} \in \mathbb{Z}^m} \exp\left(\frac{-|\boldsymbol{\tau} - \boldsymbol{\tau}' - 2\pi\mathbf{k}|^2}{2\sigma(t)^2}\right)$$

Sampling from this distribution amounts from sampling from a normal distribution in \mathbb{R}^m and then modding out by units of 2π .

3.3.2 Diffusion on SO(3): orientations in three dimensions

The manifold SO(3) is the set of 3×3 orthogonal matrices with determinant 1, and so they are used to represent rigid rotations of \mathbb{R}^3 or the orientation of three-dimensional objects. Diffusing on SO(3) can be useful during generation when the structure being diffused is not spherical and properties are dependent on its orientation – for example a ligand or the residue of a protein. The transition kernel for the VE formulation is given by the IGSO(3) distribution [39], which is easily computable via a series expansion.

3.3.3 Direct product of manifolds

More complicated manifolds can be built from the direct product of simpler manifolds. The VE forward process diffuses each coordinate independently, and so for direct product the diffusion can be carried out separately on each component manifold. This allows for diffusion across multiple coordinates: for instance, diffusing the position and orientation of n particles amounts to diffusing on the manifold $\mathbb{R}^{3n} \times \text{SO}(3)^n$, for which we know each of the transition kernels.

3.4 Low-temperature sampling

A common problem with training generative models is *overdispersion*. When this occurs, the coverage of the modes of an underlying distribution is emphasized more than sample quality, leading to poor quality in the samples. This can be particularly deleterious when using generative models for predictions. It is common to use modified sampling to sacrifice diversity for higher-quality. See for instance shrunken encodings in normalizing flows [40].

Low-temperature sampling of a distribution is an attractive way to combat overdispersion. That is, if $p(x)$ is the original distribution, sampling instead from $\frac{1}{Z}p(x)^\lambda$, where Z is a normalizing factor and $\lambda > 0$ is an inverse temperature parameter, will emphasize high likelihood areas of the distribution. Taking $\lambda \rightarrow \infty$ will lead the distribution to concentrate around the global maximum of $p(x)$. This process is analogous to lowering the temperature for a thermodynamic system so that enthalpy is emphasized over entropy. However, low-temperature sampling in many cases is intractable or requires expensive Markov chain Monte Carlo (MCMC) simulations to compute.

For diffusion models, it is tempting to simply increase the score and decrease the noise, but doing this does not give the correct distribution and is generally ineffective [2]. Ingraham et al. demonstrate how to derive an approximate scheme in the case of a normal distribution [41]. One can then approximate the perturbed score function $\mathbf{s}_{\text{perturb}}$ by multiplying the original score function \mathbf{s} by a time-dependent constant λ_t : that is,

$$\mathbf{s}_{\text{perturb}}(\mathbf{x}, t) \approx \lambda_t \mathbf{s}(\mathbf{x}, t).$$

Replacing \mathbf{s} with $\mathbf{s}_{\text{perturb}}$ leads to new reverse diffusion SDE that one can use to sample the low-temperature distribution. This approximating only holds in the case of a Gaussian distribution for p_{data} , and so applying the rescaling to arbitrary distribution will not lead to a proper reweighting. However, mixing the low-temperature reverse SDE with a Langevin SDE allows for proper sampling of a generic distribution. For more details, we refer readers to [41, Appendix C].

4 Applications

Applications for diffusion models can be roughly divided into two categories: generation/design and prediction. Methods between these two categories are similar, but the goals are different in terms of sampling the underlying distribution. For generative applications, the goal is to faithfully sample the distribution. This means not only having accurate samples but also having good coverage of all modes. Design tasks are usually downstream from generation task, where one conditionally samples the distribution of interest. For predictive applications, the goal is to sample the most likely point in the probability distribution. This tends to correspond with an optimization goal, e.g., minimizing the total energy of a system.

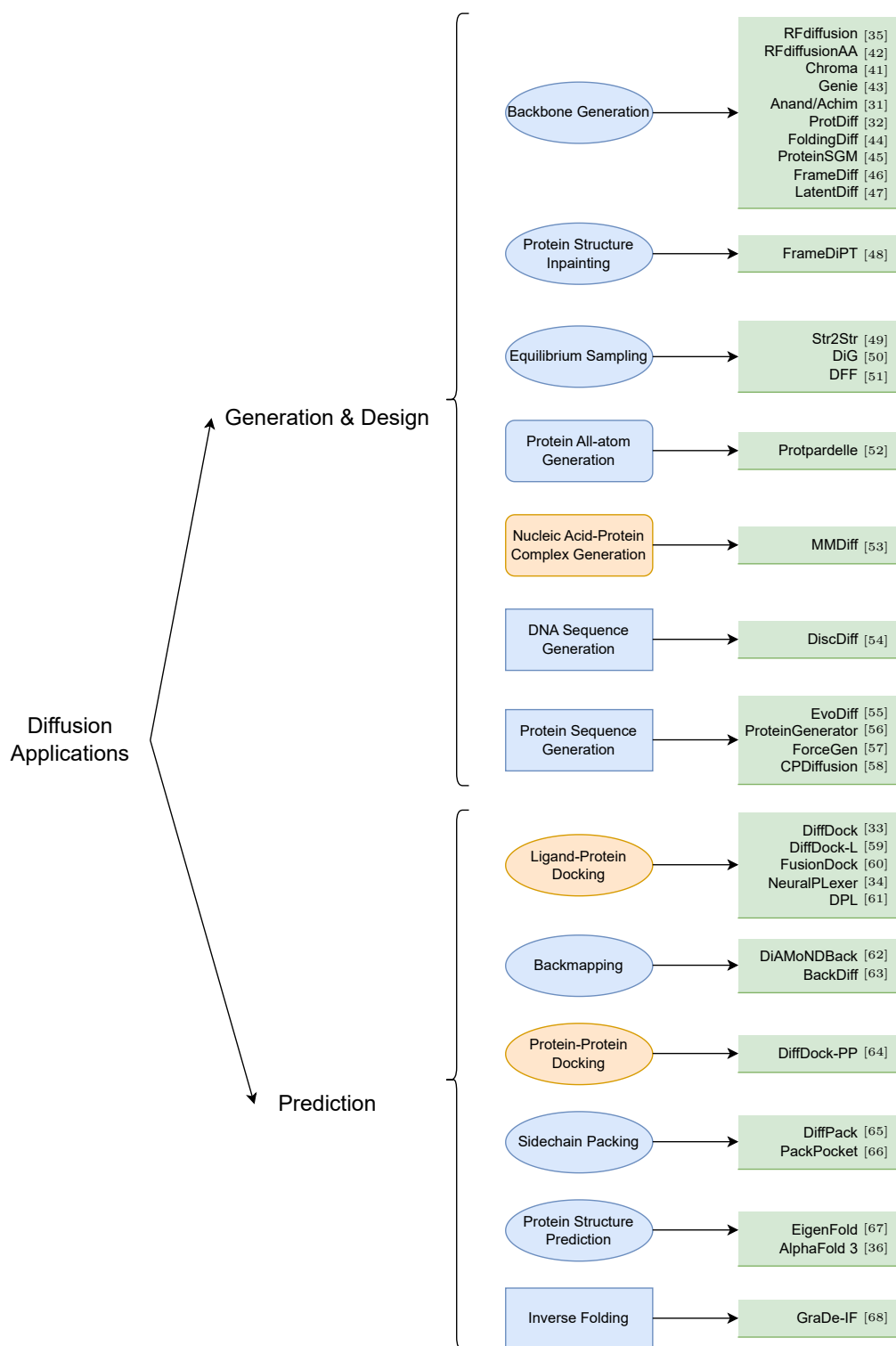


Figure 4: Summary of diffusion application for the generation and prediction of biomolecules. Ellipses are used for structure generation/prediction; rectangles for sequences; and rounded rectangles for co-generation methods. Blue shapes represent monomeric applications while orange shapes represent polymeric/complex applications.

This classification is not a strict binary, but rather represent two ends of a spectrum for sampling a distribution. There is a tension between sample *diversity* (how well a method covers all modes of a distribution) and sample *quality* (the likelihood of samples from a distribution), and there may be cases where one might sacrifice sample diversity for better quality or vice versa. For instance, we discussed how low-temperature sampling gives a controlled way to ignore smaller modes in the distribution to instead focus on more likely points. Even in prediction cases, where a single answer is desired, diversity can still be beneficial. Diversity of sampling can benefit prediction when (a) there are multiple plausible solutions, (b) there are close modes which must be discriminated or (c) a measure of flexibility or certainty is needed.

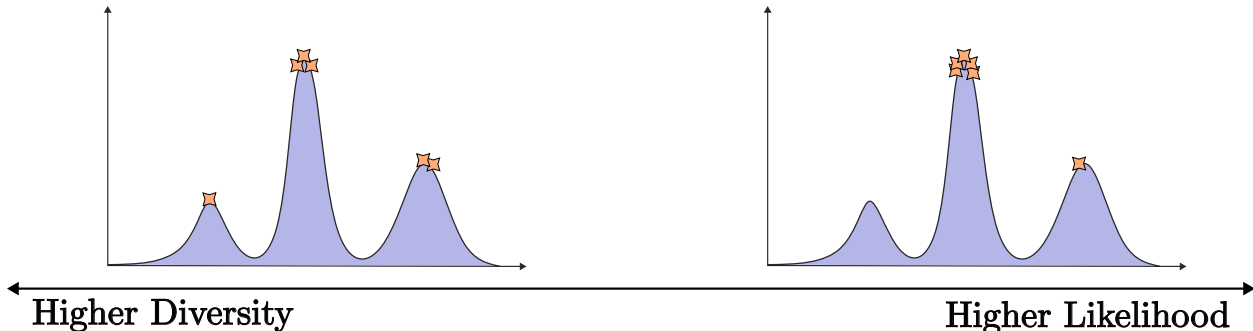


Figure 5: The difference between generation tasks and prediction tasks is how samples are to be drawn from the distribution. On the one hand, generation tasks value faithful sampling of the distribution and the sampling of all modes. On the other hand, prediction tasks value only the most likely outcomes from a distribution. The left- and right-hand plots above show this dichotomy between generation and prediction, respectively. Generated samples from the methods are shown in orange stars.

4.1 Generative modeling

Diffusion models are particularly useful for generating samples from a high-dimensional distribution, and so it is natural to apply them to the problem of creating plausible molecular structures. Furthermore, conditional diffusion allows for additional constraints to be added to the generation process, allowing for the design of proteins. Despite the recentness of the techniques, there have already been significant results. Many results focus on generating the backbone of the protein sequence (for example the locations of the $C\alpha$ atoms), and so this direction will be the main focus of this section.

4.1.1 Benchmarking

The ability of generative models to effectively sample the desired distribution is typically measured in three aspects: sample quality, sample diversity, and novelty. *Sample quality* looks at whether the generated samples are likely to come from the underlying distribution. *Sample diversity* looks at whether the distribution of samples reasonably spans the entirety of the underlying distribution. *Novelty* is a measure of how well the model generalizes from the training set; a model that simply memorizes the training data would do well with quality and diversity, but would not be able to produce new samples from the distribution.

To measure the quality of generated protein structures, one needs to determine whether a polypeptide chain has a native conformation matching the generated structure. By design, the generated structures are novel and thus cannot be directly compared with previous structures. Validating these structures experimentally is time-intensive, and so *in silico* methods for determining the structure – such as AlphaFold2 [17] and ESMFold [69] – are employed to evaluate the samples. *Self-consistency* of a method is the measure of whether a sequence can be found and independently folded into the generated structure. For many models, no sequence is generated and so a reverse folding method, such as ProteinMPNN [70], must first be used to find a number of plausible sequences. The self-consistency score is computed by comparing the folded structure with the generated structure and taking the closest comparison. The self-consistency TM (scTM) score computes the TM score between the generated backbone and each folded backbone and returns the highest

result. Another choice is the self-consistency RMSD (scRMSD) score which similarly compares structures using the backbone RMSD and returns the smallest result. The scRMSD is a more stringent requirement, and is a stricter measurement of designability. A protein is said to be *designable* if its scRMSD is less than 2 Å or its scTM score is greater than 0.5.

Assessing diversity and novelty is more straight-forward since this only involves comparisons with the generated and known structures. The average pairwise TM score among the generated structures measures the diversity of the sampling, and the maximum TM score of the generated structure and the training set measures the novelty of the sampling. Other qualitative measures of assessing the model exist as well. For unconditional generation, comparing the distribution of relevant statistics (e.g. dihedral angles and secondary structure) can help determine whether the sampling does not well approximate the underlying distribution.

4.1.2 Backbone generation models

Trippe et al. created a generative model for the C α backbone of proteins with a specific focus on controllable generation for the motif-scaffold problem [32]. Diffusion was carried out on the Cartesian coordinates and used an $E(3)$ equivariant score network. Despite producing plausible protein structures, generally the backbones were not designable. Furthermore, the equivariance of the network to reflections produced incorrect left-handed α -helices, and so the model did not respect the chirality of the proteins. Wu et al. diffused on the internal angles of the protein backbone in order to create a generative model that respects chirality [44]. Again, the generated proteins were plausible and had distributions of secondary structures similar to native proteins, but most generated backbones were not designable.

ProteinSGM was one of the first models to be able to generate highly designable protein backbones [45]. The diffusion is carried out on the six-dimensional space of inter-residue coordinates as defined in trRossetta [71], using the VE SDE formulation. Protein backbones are obtained from coordinates using an adaptation of the trRossetta minimization method, which enables generation of realistic structures. ProteinSGM is able to generate proteins up to length 128 with scTM of 90.2%, versus 11.8% and 22.7% as reported by [32] and [44], respectively.

Ingraham et al. developed Chroma, which generates backbones by diffusing on the C α atoms [41]. The backbones generated are more likely to be designable than the previously mentioned methods, with around 50% being designable by their criterion. Notable features of their model include (1) choosing a covariance structure of the initial distribution to replicate the statistics of realistic protein backbones (such as radius of gyration), (2) a random graph neural score network to maintain subquadratic computational time, and (3) an annealed sampling scheme that allows the model to sample from $\frac{1}{Z}p(x)^\lambda$ without retraining. Furthermore, the programmability of the model and code is emphasized in the paper. That is, several conditioners are created to allow for a wide range of conditions for protein generation, such as on the three-dimensional shape and point symmetries of the final structure. The generated protein structures are diverse and cover all of natural protein space.

Other recent attempts at diffusion models for protein generation carry out the diffusion process on the coordinates and orientations of the backbone atoms. That is, for n atoms, diffusion will be carried out on $\mathbb{R}^{3n} \times \text{SO}(3)^n \simeq \text{SE}(3)$. This allows the models to reason about the three-dimensional structure of the protein during the generation step while retaining angular information between residues so that chirality is respected. This paired with SE(3) equivariant networks like IPA have been particularly successful.

The most salient example of this method is RFdiffusion, which is considered the gold standard of backbone generation [35]. As argued by the authors, previous models lacked deep understanding of protein structure, and so taking advantage of structure predictions methods could allow for better sample quality. In particular, pretraining using the weights from RoseTTAFold [72] provided an enormous benefit to the diffusion model. RFdiffusion has high designability of unconditionally generated proteins, with independent benchmarking showing over 95% of moderately sized backbones being designable [73, 43] and some of the protein designs being experimentally verified [35]. Furthermore, the model is capable of conditional generation of proteins, such as producing oligomers with point symmetries and functional-motif scaffolding. Recent work has been done on expanding RFdiffusion’s capabilities to more general biomolecular tasks. RoseTTAFold All-atom (RFAA) [42] expands RoseTTAFold’s by including atomic-level inputs for other biomolecular components. This allows RFAA to more accurately predict protein structure in the context of assemblies of molecules. RFdiffusionAA (similar to the original RFdiffusion) uses the pretrained weights of RFAA to develop a

protein backbone generation model. Thus RFdiffusionAA can generate protein structures conditioned on small-molecule binders. Designs from RFdiffusionAA were experimentally validated and were shown to bind with the target molecules.

Other models have used SE(3) diffusion to get designable backbones without the need to pretrain. Anaand and Achim were able to generate plausible protein structures diffusing on SE(3)² and capture realistic distributions of secondary structures [31]. The diffusive process in this case was approximated by random interpolations in the space. FrameDiff uses a principled approach of diffusing on SE(3) where the loss is given by denoising score matching (as opposed to a Frobenius norm used in [35]). The score network uses IPA to capture spatial relationships while a transformer captures interactions along the protein chain. The model is able to generate designable backbones (using the scTM metric) about 75% of the time, while still maintaining diversity and novelty of the samples. This model is also extendable to the protein in-painting problem, as demonstrated by FrameDiPT [48].

Lin and AlQuraishi carry out a similar idea by using SE(3) equivariant network [43]. The forward diffusion process is carried out on the coordinates on the C α atoms while the backward process uses coordinate frames to predict the noise displacements at each step. This allows for a cheaper noising process while allowing the full reasoning of IPA when generating samples. The authors demonstrate improved designability and diversity of tertiary structures compared with FrameDiff (although FrameDiff showed better diversity of secondary structure elements).

Method	Designability % scRMSD < 2.0 Å \uparrow	Diversity TM-Score \downarrow	Novelty % PDBTM < 0.5 \uparrow	Number of Parameters
RFdiffusion	0.904	0.2894	0.3750	59.8 M
Chroma	0.728	0.2779	0.3198	32.4 M
FrameDiff	0.484	0.2912	0.157	17.4 M
Genie	0.668	0.2674	0.5069	4.1 M

Table 1: Benchmarking of backbone generation models on unconditional generation.

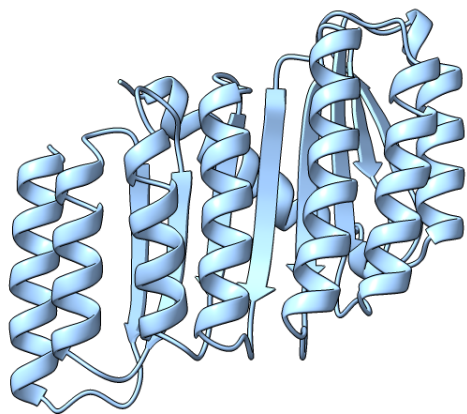
For convenience, we provided original benchmarking of backbone generation methods. The results are given in table 1 and further details of the benchmarking are provided in appendix A.1. Notably, RFdiffusion performs the best in designability, which matches the benchmarking done in other works. Genie performs well with diversity and novelty, despite its relatively small size compared to the other models. One should note that there is a tradeoff between designability and diversity/novelty: prioritizing designability will lead to proteins with more stable structures but may bias toward predictable designs (e.g. an overemphasis on α -helices). However, RFdiffusion still performs well on all metrics, even given its high designability. The strength of RFdiffusion can likely be credited to using pretrained weights from RoseTTAFold, which gives useful information about protein tertiary structure.

4.1.3 Other generative models

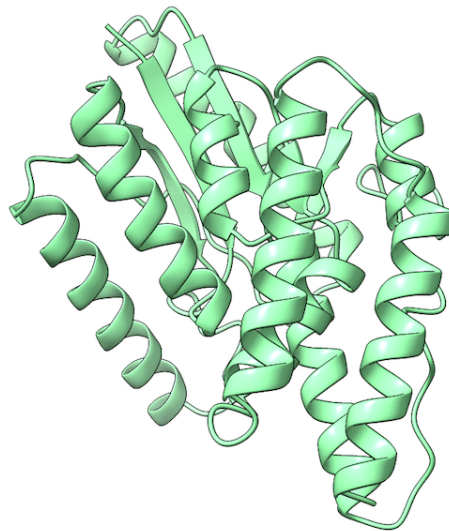
Although generating proteins based on backbones coordinates is a popular choice, other approaches have been attempted. One deficit to focusing on coordinates is that conditional generation based on sequence information is not possible: the backbone methods above only consider structural information and obtain the sequences via a reverse folding method. Thus diffusing in *sequence* space could be useful for conditioning on sequence information. Up to this point, we have only discussed diffusion on continuous spaces (either Euclidean space or a manifold), while diffusing on sequences requires being in a discrete space. One option for bringing diffusion to discrete space is to simply embed categorical information into continuous (e.g. using a one-hot encoding scheme) and then performing a traditional diffusion. A more principled options is to create a diffusion scheme for discrete data. For instance, Discrete Denoising Diffusion Probabilistic Models (D3PMs) describe a corruption process for discrete data that is analogous to Gaussian noise [74].

This more principled approach was taken by the authors of EvoDiff, which is a protein sequence generation model [55]. EvoDiff carries out discrete diffusion in a method similar to D3PM, but the authors found it

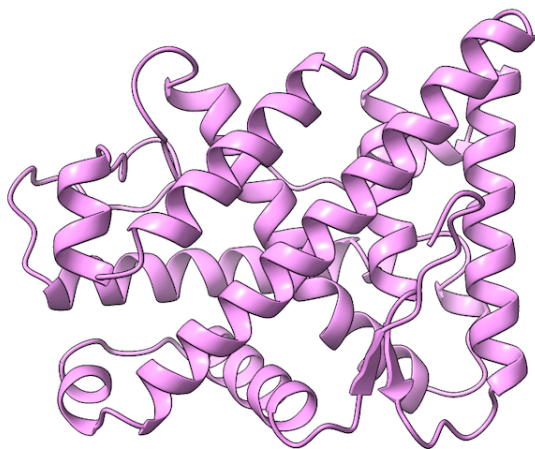
²More accurately the diffusion took place on $\mathbb{R}^3 \times \text{SU}(2)$, where quaternions are used to represent orientation.



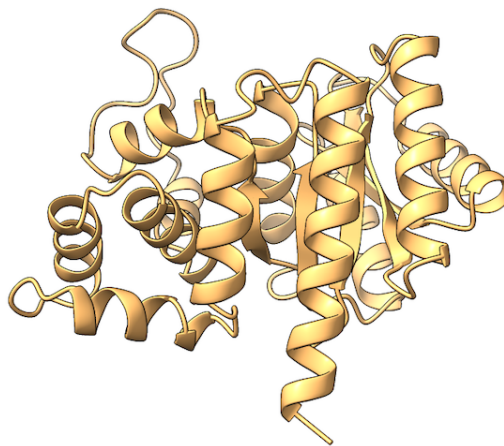
(a)



(b)



(c)



(d)

Figure 6: Example protein backbone generated from diffusion methods. Each backbone is 250 residues long: (a) RFdiffusion [35]; (b) Chroma [41]; (c) FrameDiff [46]; (d) Genie [43].

more successful to generate the sequence autoregressively. The model demonstrates good coverage of protein sequence space. By embedding the sequences with ProtT5 [75] and computing the Fréchet distance between the generated set and the test set, the authors show that EvoDiff provides better coverage than other protein language models [76] and RFDiffusion [35]. EvoDiff is able to generate proteins with intrinsically disordered regions, which is something that other structure-based diffusion methods struggle to do. Furthermore, it is also possible to condition on MSA data to generate other members of a protein family without retraining. Overall, many of the strengths of EvoDiff are orthogonal to those of structure-based diffusion.

Protein Generator is another method that opts to diffuse over sequence space to generate protein structures [56]. However, the diffusion process is carried out in continuous space as standard DDPM, where the amino acid sequence is embedded via a one-hot encoding. Structures are simultaneously generated by fine-tuning RoseTTAfold [72] to accept noisy sequences and diffusion times³. This method creates sequences alongside a physically plausible three-dimensional structure. This also allows for the conditional generation based on sequence and structure.

Research has also been focused on sequence generation of proteins with predefined functions. For instance, ForceGen uses a pretrained protein language (pLM) model to diffuse in probability space [57]. The authors were particularly focused on generating proteins which matched mechanical folding responses. To accomplish this, they curated a dataset consisting of protein sequences as well MD simulation data of the force required to stretch a protein. Samples are then generated by reversing diffusion in probability space with the force data as a conditioner. The pLM is then used to decode the sequence for the final prediction. The generated sequences were tested by obtaining the three-dimensional structure via OmegaFold [77] and then simulating the mechanical unfolding. It was shown that the generated sequences do produce responses close to the conditioned mechanical response. Another example is CPDiffusion, which is a DDPM treating sequences as categorical data embedded in Euclidean space [78]. In the study, the authors use CPDiffusion to generate novel programmable endonucleases. The designed proteins (after an initial screening) were validated experimentally, with all 27 being soluble. Furthermore, some of the proteins demonstrated desired properties, with 24 of them displaying DNA cleavage activity and most having enhanced enzymatic activity compared to the template protein.

Another novel diffusion method was used in the development on LatentDiff [47]. As the name suggests, diffusion is not carried out in coordinate space but rather in a latent space. Inspired by image generation methods like StableDiffusion [79], Fu et al. create an SE(3) autoencoder to downsample the geometry of the protein as well as upsample to recover the protein coordinates. Protein generation is carried out by reversing diffusion in the latent space and then upsampling to retrieve the predicted protein. In benchmarking, the method outperforms other small-protein generation methods, such as FoldingDiff, in designability with comparable (but slightly worse) results to FrameDiff. However, its sampling speed is around 64 times faster than FrameDiff, likely due to the reduced dimensionality of the latent space.

Protpardelle differs from the backbone generation methods in that it generates proteins at an all-atom resolution [52]. An obstacle to all-atom generation is that the number and types of atoms are determined exactly by the amino acid sequence, so making a choice on the coordinates to diffuse will also determine the amino acid sequence and thus the final structure of the protein. To address this, diffusion is carried out on a “superposition” of possible structures. That is, the positions of atoms for any choice of amino acid are tracked during diffusion, allowing the model the flexibility to decide the sequence during the generation process. On the standard benchmarks, Protpardelle does quite well. In particular, its scRMSD score is about 90% for small proteins and around 70% for proteins around 300 amino acids in length. Also, because the model generates an all-atom representation, it is possible to condition generation on side-chain information. However, improvements in conditional generation are needed as the model is prone to ignoring the conditioning information.

While an overwhelming amount of work has been done on the generation and design of proteins, relatively less attention has been paid to other biomolecules. However, there have been some recent efforts to bring diffusion methods to DNA and RNA generation.

For instance, DiscDiff is a latent diffusion model for generating DNA sequences [54]. A variational autoencoder is trained to first take DNA sequences into a latent space. Then a diffusion model is trained in latent space to produce samples. One notable change that the authors make is during the decoding step.

³This method of structure generation echoes RFDiffusion, which uses pretrained weights from RoseTTAfold to guide training.

Often with latent diffusion models, errors may be introduced when moving from latent space to sequence space. The authors hypothesize that the latent variable captures the global information of the sequence well but that there may be regions in the sequence with lower certainty. To address the authors introduce the Absorb-Escape method, where a pretrained autoregressive model for DNA sequences is used to correct nucleotides with lower certainty. When benchmarking against other sequence generation methods trained on the DNA task, it achieved state-of-the-art results without post-conditioning and did even better with Absorb-Escape.

Another attempt of bringing diffusion models to other biomolecules can be seen with MMDiff [53]. This model jointly generates sequences and structures of nucleic acid and protein complexes. Many of the methods are directly inspired by the work of diffusion models applied to proteins. The diffusion takes place in $SE(3)$ with coordinate frames for each of the residues of the protein and RNA/DNA structures, similar to that used by Yim et al. [46]. Sequences are simultaneously generated by embedding them into continuous space via a one-hot encoding, as done by Lianza et al. for Protein Generator [56]. Benchmarking proceeds analogously to protein generation, where designability, diversity, and novelty are assessed. However, MMDiff fails to achieve high designability. For instance, the percentage of designable protein-nucleic acid complexes is 0.74% (versus 0.37% for random generation). The method does marginally better with the generation of nucleic acids only, with 8.67% being designable (1.33% for random generation). The authors suggest that the key to improvement is more diverse and high-quality training data. This highlights the current challenges in directly transferring structural generation models to the problem of RNA and DNA generation.

4.1.4 Molecular dynamics and ensemble generation

Molecular dynamics simulations is an important tool for computational biology. It sees uses in the refinement of predictions and the study of dynamics of biomolecules [80, 81, 82, 83, 84, 85, 86]. Typically, simulations are carried out using Langevin dynamics and a prescribed potential energy function. However, computation of a conventional energy function is expensive (usually quadratic in the number of particles), and so simulating the dynamics on a suitably long time-scale is infeasible. Generative models have the ability to speed up these computations by directly sampling the distribution of future states conditioned on the current state. This has been applied to the simulation of molecules with diffusion models and other generative models [87, 88]. However, this direction has not been thoroughly explored for the simulation of protein dynamics.

Lu et al. made progress in this direction with the introduction of Str2Str, a model for sampling protein conformations [49]. The method shares similarities to simulated annealing, where the temperature for MD simulations is raised to overcome energetic barriers. Here a structure is perturbed by diffusion, and then the process is reversed to sample a new conformation of the protein. The noising process is carried out in $SE(3)$ as described by Yim et al. [46] and the score network is given by a variant of IPA [17]. Str2Str is able to recapture many of the statistics of the equilibrium distributions of fast-folding proteins in negligible amount of time compared to direct MD simulation (510 GPU seconds versus over 160 GPU days, respectively.)

A similar approach was carried out by Zheng et al. with the development of the Distributional Graphormer (DiG) [50]. This model samples the equilibrium distribution of molecular systems using a diffusion model, where the score architecture is given by a Graphormer. In this work, the equilibrium distribution of proteins is used during training and validation. Again, diffusion is carried out over frame data in $SE(3)$ using the VE formulation of the SDE. One notable addition to the typical diffusion model is the use of physics-informed diffusion pre-training (PIDP). Since MD simulation are expensive to compute, the authors sought a method to utilize prior energy functions to train the score model. The main idea is to enforce that the score network satisfies the corresponding Fokker-Plank equation – a partial differential equation which governs the value of the score through the diffusion process – and the initial condition given by the gradient of the prior energy. The PIDP does not require samples from the equilibrium distribution since information from the energy function will enforce the correct distributions. A tractable number of samples can be selected during this process since the equilibrium distribution lies on a much lower dimensional manifold than the latent space. DiG is shown to recapture protein equilibrium distributions, as well as generate plausible transition paths between conformations.

A related direction is the training of coarse-grained models for proteins. The free-energy landscape for an all-atom representation of a protein is rough and difficult to simulate, so coarse-grained models look to simplify the simulations by combining particles. The training of coarse-grained models is typically done

through variational force matching, where the forces on the virtual particles are chosen to match the expected force before the coarse-graining process. However, this process is data-inefficient since the coarse-graining maps many configurations to the same state and so forces must be averaged out over those configurations. An alternative method is using relative entropy, but this requires resampling the coarse-grained distribution during training. Flow-matching is a more data-efficient method of training a coarse-grained model [89], which first uses a generative model to learn the equilibrium distribution of a protein that then is used to determine the forces of the model. This method is built on by Arts et al. who train a generative and coarse-grained model simultaneously using a denoising diffusion generative model [51]. Similarly to flow matching, training does not require the recording of forces. The coarse-grained model and sampler are able to recapture the equilibrium distribution of the proteins on which they are trained. The training scheme shows promise in terms of scaling to longer proteins.

4.2 Predictive modeling

Diffusion models being generative models are traditionally designed to sample the whole probability distribution they are trained on. However, there has been success with using diffusion models to predict the solution to regression and/or optimization problems with a single solution. Non-generative machine learning methods sometimes struggle to account for uncertainty and thus try to minimize the expected error at the cost of realistic predictions (see [33, §3] for an example). A generative model instead handles the uncertainty by sampling over all possibilities, giving a more accurate representation of the likely solution.

For generating a single prediction, one can repeatedly sample from the diffusion model and then choose the “best” sample. A typical strategy for making the final choice is training a separate confidence model which would rank each of the samples based on the confidence of being the optimal solution. A training-free alternative would be to use a likelihood estimate or evidence-based lower bound (ELBO) to determine the most likely sample from the distribution.

Following this strategy, several diffusion models have been applied to prediction problems and have achieved state-of-the-art results.

4.2.1 Protein side-chains

The protein side-chain packing problem focuses on the case where the backbone of a protein is fixed and asks for the positions of its side-chain atoms. Traditional methods for solving the problem involve searching the space of positions for the side-chains using rotamer libraries and comparing energies [90, 91, 92, 93, 94, 95, 96, 97]. Due to the complexity of the energy landscape and the number of possible conformations of the side-chains, this process can be time-intensive. Machine-learning methods aim to speed up this process while maintaining precision. Methods such as AttnPacker [98] predict the positions of the side-chain atoms but do not account for bond lengths and angles. Other machine learning methods treat side-chain packing as a regression problem and do not model the diversity of possible conformations in the energy landscape [99, 12].

DiffPack is a diffusion-based model for side-chain packing that predicts the torsional angles, χ_1, χ_2, \dots , of each side-chain [65]. Ideal bond lengths and angles are assumed for the side-chain atoms, so that the degrees of freedom are greatly reduced and the samples produced have natural bond lengths and angles. The diffusion process is carried out on \mathbb{T}^n , where a sample corresponds to a choice of torsional angles for the side-chains. One notable change in the diffusion process is that the angles are sampled autoregressively: χ_1 is first sampled, followed by χ_2 and so on. Since the value of χ_1 affects the coordinates of atoms further down the chain, sampling all angles simultaneously can lead to excess steric clashes due to the sensitivity of earlier angles on coordinates. Using an autoregressive generation process mitigates this effect because the model can self-correct for earlier choices of angles. A confidence model is trained along side the diffusion model in order to score the sampled conformations. During inference, multi-round sampling and annealed temperature sampling are used to choose conformations with lower energies. DiffPack is able to achieve state-of-the-art performance in the mean absolute error of the predicted torsional angles when compared to other machine learning approaches to the side-chain packing problem. Diffpack’s reported results are given in tables 2 and 3. For details on the benchmarking, see appendix A.2.

A related problem to side-chain packing for *apo* protein structures is determining the conformations of

Method	ANGLE MAE ° ↓				ANGLE ACCURACY % ↑			ATOM RMSD Å ↓		
	χ_1	χ_2	χ_3	χ_4	All	Core	Surface	All	Core	Surface
SCWRL	27.64	28.97	49.75	61.54	56.2%	71.3%	43.4%	0.934	0.495	1.027
FASPR	27.04	28.41	50.30	60.89	56.4%	70.3%	43.6%	0.910	0.502	1.002
RosettaPacker	25.88	28.25	48.13	59.82	58.6%	75.3%	35.7%	0.872	0.422	1.001
DLPacker	22.18	27.00	51.22	70.04	58.8%	73.9%	45.4%	0.772	0.402	0.876
AttnPacker	18.92	23.17	44.89	58.98	62.1%	73.7%	47.6%	0.669	0.366	0.775
DiffPack	15.35	19.19	37.30	50.19	69.5%	82.7%	57.3%	0.579	0.298	0.696

Table 2: Comparative evaluation of DiffPack and prior methods on CASP13 as reported in [65].

Method	ANGLE MAE ° ↓				ANGLE ACCURACY % ↑			ATOM RMSD Å ↓		
	χ_1	χ_2	χ_3	χ_4	All	Core	Surface	All	Core	Surface
SCWRL	33.50	33.05	51.61	55.28	45.4%	62.5%	33.2%	1.062	0.567	1.216
FASPR	33.04	32.49	50.15	54.82	46.3%	62.4%	34.0%	1.048	0.594	1.205
RosettaPacker	31.79	28.25	50.54	56.16	47.5%	67.2%	33.5%	1.006	0.501	1.183
DLPacker	29.01	33.00	53.98	72.88	48.0%	66.9%	33.9%	0.929	0.476	1.107
AttnPacker	25.34	28.19	48.77	51.92	50.9%	66.2%	36.3%	0.823	0.438	1.001
DiffPack	21.91	25.54	44.27	55.03	57.5%	77.8%	43.5%	0.770	0.356	0.956

Table 3: Comparative evaluation of DiffPack and prior methods on CASP14 as reported in [65].

side-chains for ligand-docking problems. The native structure of proteins do not account for the the complex flexibility of proteins, which adapt their structure to their respective molecular binders. Thus there is demand for methods which take this flexibility into account. PackDock seeks to incorporate this flexibility to improve on ligand-protein docking predictions [66]. The authors note that the dynamics of the protein-ligand process are commonly described by two mechanisms: conformational selection and induced fit. A torsional diffusion method – called PackPocket – is introduced to sample multiple possible conformations for the side-chains, either with or without the ligand. This is carried out in conjunction with a docking algorithm to sample ligand conformations in the binding pocket (Vina [100] is used by the authors, but any docking method can be used). PackDock was shown to improve docking predictions when considering *apo* structures or *holo* structures form non-homologous ligands.

4.2.2 Protein structure prediction

Diffusion models have also been applied to the problem of predicting the native structure of proteins. In particular, EigenFold predicts the coordinates of the $C\alpha$ atoms of a protein [67]. Diffusion is carried out on the Cartesian space \mathbb{R}^{3n} , but the diffusion process is defined so that the prior distribution uses a Harmonic potential for the relative distances of points. This guarantees that diffused points do not separate too far and that relative distances more closely reflect observed bond lengths. Thus the prior distribution models more realistic molecular conformations, but the stiffness of the diffusion process requires the SDE be carried out with a basis of eigenvectors. An estimated ELBO is used *in lieu* of training a score model. The results reported in table 4 are modest compared to established machine learning approaches such as AlphaFold2 and ESMFold [17, 69] (see appendix A.3 for details). One benefit to using a generative model over a single-structure prediction methods is that generative models can naturally capture conformational diversity of a protein. If a protein is flexible, then sampling the distribution of conformations should result in different possible poses. Eigenfold shows some moderate results in this direction, with a slight correlation between the diversity of samples and the flexibility of the protein. Overall, the model demonstrates the possibilities of diffusion models to the problem of predicting native structures.

A recent development in protein-structure prediction was the announcement of AlphaFold 3 (AF3) [36].

The main improvement of AF3 over AF2 [17] and AlphaFold-Multimer [101] is its capability of modeling general molecules. In particular, the accelerated review paper cites state-of-the-art results in ligand-protein complex predictions and advancements in protein-RNA modeling compared to other automated methods. To accommodate the more general modeling of biomolecular interactions, the generation process was switched to an all-atom framework that can generalize the construction process of proteins and other molecules that do not have amino acid nor nucleic acid residues. Since frames and invariant point attention cannot be used in this case, the structure module of AF2 was changed to a diffusion module in AF3. The diffusion module takes the embedding information created by AF3 in order to determine the atom positions of the proteins and other molecules, where the generation process follows a standard iterative process of removing Gaussian noise from a sample. One notable difference between AF3 and other applications of diffusion to biomolecules is the lack of invariance/equivariance to rotations and translations in the architecture. Instead, data augmentation is used to achieve equivariance.

A related but narrower problem is that of backmapping: the task of determining an all-atom configuration from a coarse-grained representation. Data-driven approaches to the problem seek to accurately reconstruct the protein while avoiding un-physical results such as clashes. While some methods are deterministic, an additional goal would be to capture the diversity of different possible all-atom configurations in a thermodynamically consistent way. Previous state-of-the-art methods, used generative models such as GANs [1] and variational auto-encoders (VAEs) [102]. In particular, GenZProt uses a VAE to backmap a $C\alpha$ trace to a full-atom resolution while still generalizing to molecules outside the training set. Researchers have begun to use diffusion models to generate backmapping samples. DiAMoNDBack, for instance, uses diffusion to backmap $C\alpha$ traces [62]. The backmapping is done residue-by-residue in an autoregressive fashion, which lends to a more transferable model. Another approach to this problem is BackDiff, which more generally backmaps any coarse-grained representation [63]. Determining the position of heavy-atoms given the coarse-grained atoms is treated as an imputation problem, and training is done by randomly choosing heavy atoms (apart from the $C\alpha$ atoms) to mask. Conditioning on auxiliary variables and enforcing bond lengths and angles are handled during generation using a manifold constraint. Both DiAMoNDBack and BackDiff are shown to outperform GenZProt in terms of accuracy of full-atom reconstructions, diversity of samples, and the avoidance of clashes and un-physical bond lengths and angles.

4.2.3 Inverse protein folding

As opposed to structural prediction methods, the inverse folding problem looks at determining an amino acid sequence given a protein’s $C\alpha$ backbone. GraDe-IF applies a discrete diffusion model to the inverse folding problem [68]. The diffusion is carried out in the categorical space of amino acid types using the D3PM framework [74]. Notably, the authors use the Blocks Substitution Matrix (BLOSUM) [103] to create the transition matrix for the noising step. This allows the model to explore closely related amino acids during the latter stage of the denoising process instead of random, unrelated residue types. The score network is given by an adaptation of an equivariant graph neural network (EGNN) [38] to account for the roto-translational invariance of the problem. The model outperforms other inverse folding methods in the authors’ benchmarking as reported in table 5. Details of the benchmarking can be found in appendix A.4.

	RMSD $_{C\alpha}$ ↓	TMScore ↑	GDT-TS ↑	IDDT $_{C\alpha}$ ↑
ALPHAFOLD2	3.30 / 1.64	0.87 / 0.95	0.86 / 0.91	0.90 / 0.93
ESMFOLD	3.99 / 2.03	0.85 / 0.93	0.83 / 0.88	0.87 / 0.90
OMEGAFOLD	5.26 / 2.62	0.80 / 0.89	0.77 / 0.84	0.83 / 0.89
ROSETTAFOLD	5.72 / 3.17	0.77 / 0.84	0.71 / 0.75	0.79 / 0.82
EIGENFOLD	7.37 / 3.50	0.75 / 0.84	0.71 / 0.79	0.78 / 0.85

Table 4: Single-structure prediction accuracy of EIGENFOLD and baseline methods on CAMEO targets under 750 residues from Aug 1–Oct 31, 2022. All metrics are reported as mean / median. Table from [67]

Model	Perplexity ↓			Recovery Rate % ↑			CATH version	
	Short	Single-chain	All	Short	Single-chain	All	4.2	4.3
STRUCTGNN	8.29	8.74	6.40	29.44	28.26	35.91	✓	
GRAPHTRANS	8.39	8.83	6.63	28.14	28.46	35.82	✓	
GCA	7.09	7.49	6.05	32.62	31.10	37.64	✓	
GVP	7.23	7.84	5.36	30.60	28.95	39.47	✓	
GVP-large	7.68	6.12	6.17	32.6	39.4	39.2		✓
ALPHADESIGN	7.32	7.63	6.30	34.16	32.66	41.31	✓	
ESM-IF1	8.18	6.33	6.44	31.3	38.5	38.3		✓
PROTEINMPNN	6.21	6.68	4.57	36.35	34.43	49.87	✓	
PIFOLD	6.04	6.31	4.55	39.84	38.53	51.66	✓	
GRADE-IF	5.49	6.21	4.35	45.27	42.77	52.21	✓	

Table 5: Recovery rate performance of **CATH** on zero-shot models. Table taken from [68]

4.2.4 Protein complexes

Ligands bind to proteins and modulate their biological function, so an important step in drug design is determining where a ligand will bind to a protein. Traditionally, computational methods for this problem search for the ligand position that directly optimizes a score function [100, 14, 104]. However, due to the high-dimensionality of the space and the roughness of the energy landscape, this process can be slow and give inaccurate results. Machine learning approaches that treat ligand-binding as a regression problem significantly speed up the process but still suffer from inaccuracy due to the uncertainty in the energy landscape [105, 106]. DiffDock [33] instead treats the finding the ligand pose as a generative problem. Put simply, DiffDock samples possible ligand poses from an underlying distribution and then makes an optimal choice based on a learned confidence score. This circumvents the ruggedness of the energy landscape by enumerating multiple options instead of averaging possibilities together as done in regression-type approaches. DiffDock uses a diffusion model to sample different poses and a separate score model to determine the confidence that the RMSD is below 2 Å. The dimensionality of the search space is reduced by fixing the conformation of the protein and assuming ideal bond lengths and bond angles in the ligand. Thus the degrees of freedom are the position, orientation, and dihedral angles of the ligand. Then sampling a ligand pose is the same as sampling from the manifold $\mathbb{R}^3 \times \text{SO}(3) \times \mathbb{T}^m$, where m is the number of torsional angles. DiffDock was benchmarked on the PDBBind dataset [107] with a time split at 2019 for training and validation. On this data set, DiffDock reported state-of-the-art performance, and it retained high accuracy on computationally obtained structures. FusionDock augments DiffDock’s approach by using physics-informed priors [60].

However, the reported results tell an incomplete story of DiffDock’s strength. Some noted that the comparison to classical docking methods is unfair since traditional methods were not designed for blind docking and typically require a designated pocket to perform well [108]. When given a binding pocket, traditional methods outperform deep learning methods. But experiments demonstrated that DiffDock still excels at pocket-finding. Others have pointed out that the typical time split in PDBBind can lead to data leakage in the validation; some of the structures in the training set are similar to those in the validation set, leading to an overestimation of a model’s performance [109, 110]. Finally, many of the predictions of deep learning docking methods are physically implausible, and when accounting for docking predictions that are within 2 Å of the true structure *and* realistic, deep learning methods perform substantially worse than classical methods [111]. Recently, Corso et al. created a new benchmark set, DockGen, that removes the data leakage in terms of structure and pocket similarity [59]. In addition, they introduce DiffDock-L, a larger model trained on a bigger, augmented data set. On both the PDBBind and DockGen benchmarks, DiffDock-L outperforms all other blind docking methods. Table 6 details the results of DiffDock-L. More information on benchmarking is given in appendix A.5.

A similar framework was applied to the protein-protein docking problem with DiffDock-PP [64]. The diffusion process from DiffDock is adapted by assuming that the proteins are rigid bodies so that diffusion

Method	PDBBind		DOCKGEN-full		DOCKGEN-clusters		Average Runtime (s)
	%<2Å	Med.	%<2Å	Med.	%<2Å	Med.	
SMINA	18.7	7.1	7.9	13.8	2.4	16.4	126*
SMINA (EX. 64)	25.4	5.5	10.6	13.5	4.7	14.7	347*
P2RANK+SMINA	20.4	4.3	7.9	14.1	1.2	16.4	126*
GNINA	22.9	7.7	14.3	15.2	9.4	14.5	127
GNINA (EX. 64)	32.1	4.2	17.5	8.1	11.8	6.2	348
P2RANK+GNINA	28.8	4.9	13.8	16.2	4.7	15.3	127
EQUIBIND	5.5	6.2	0.0	13.3	0.0	13.3	0.04
TANKBIND	20.4	4.0	0.5	11.6	0.0	11.1	0.7
DIFFDOCK (10)	35.0	3.6	7.1	6.8	6.1	6.0	10
DIFFDOCK (40)	38.2	3.3	6.0	7.3	3.7	6.7	40
DIFFDOCK-L (10)	43.0	2.8	22.6	4.3	27.6	3.7	25

Table 6: Top-1 RMSD performance of different methods on the PDBBind and DOCKGEN benchmarks. Runtimes were computed as averages over the PDBBind test set. * run on CPU. Med. indicates the median RMSD. Table from [59].

takes place on $\mathbb{R}^3 \times \text{SO}(3)$ with torsional fixed. Benchmarking showed improvements in accuracy compared to other machine learning methods while being much faster than traditional search methods when computed on GPU.

NeuralPLexer is another diffusion-based method that predicts ligand-protein docking complexes [34]. Unlike previous docking prediction models, this method does not rely on the protein structure as an input but only takes the protein sequence and ligand molecular graph. NeuralPLexer is comprised of a graph-based architecture to encode molecular properties, a contact prediction module that determines the intermolecular distances, and an equivariant diffusion module that determines the structure of the complex at an atomic resolution. When applied to the blind ligand-protein docking problem (a simplification of the full complex prediction), NeuralPLexer outperformed other methods like DiffDock. The model also outperforms AlphaFold2 on protein structure prediction for structures with high flexibility and newly added protein-ligand complexes.⁴

A similar model to NeuralPLexer is the Diffusion model for Protein-Ligand complexes (DPL) [61]. Like NeuralPLexer, it does not take protein structure as an input, but only relies on the protein sequence and ligand molecular graph. Furthermore, DPL does not rely on protein backbone templates during prediction. The inputs are embedded into a single and pair representation with information from a protein language model (ESM-2) [76] and these representations are updated with Folding blocks from ESMFold [69]. Finally, and equivariant denoising network is used to generate the complex. DPL is able to generate diverse sets of complexes, but performance is limited for complexes with less data.

5 Conclusion

Diffusion models have made remarkable progress in the design and prediction of proteins, with many recent models quickly achieving state-of-the-art performance on tasks. Protein backbone generation methods, such as RFdiffusion, have demonstrated incredible success at sampling realistic and novel structures that have been validated experimentally [35]. In addition, the ability to conditionally generate structures opens up new avenues for designing proteins with desired properties. Diffusion models have also seen great success with other generation tasks, such as sequence generation/design and ensemble sampling.

They have also seen success in predictive tasks. Generative models are better at sampling many possible modes in a distribution (as opposed to regression models which average over possibilities leading to unrealistic results), which gives them an edge in some predictive tasks. Diffusion models in particular seem well suited to

⁴A recent press release claims improved performance for the newly trained NeuralPLexer2, although details have yet to be released.

searching a large-dimensional, continuous space, as partially evidenced by DiffDock’s ability to find pockets for protein-ligand docking [108].

One direction that we believe remains underexplored is the use of diffusion models for generating and predicting DNA/RNA structures. As seen with the results with proteins, diffusion models provide a potentially potent method for solving problems in this domain. Attempts at structure prediction has led to mild results [53]. Some success has been achieved with jointly modeling them with proteins ([36], for instance) where deep knowledge of protein structure can be leveraged, but there has been little success in monomeric prediction of these biomolecules alone. To this end, there are some challenges to directly applying diffusion methods: (1) there is relatively less data for nucleic acids as compared to proteins, which makes training more difficult; and (2) RNA structures are more flexible, which mirrors the difficulty with certain protein generation methods from creating intrinsically disordered regions.

It seems certain that in the coming years there will be more attention paid to diffusion models for applications involving biomolecules, but they are not without competitors in the space. Inspired by the success of diffusion, researchers have proposed other generative deep learning methods that take an iterative approach to generation. For instance, Bayesian flow networks (BFNs) are generative models which iteratively samples noised distributions in a similar way to diffusion models [112]. The sampling process consists of continually applying Bayes’ rule to flow toward a desired distribution to sample. BFNs naturally lend themselves to multimodal problems and have been used in molecular generation [113]. A more popular approach to generative modeling has been flow matching [114]. Flow matching is a subset of continuous normalizing flows where the diffeomorphism between probability distributions is given by the pushforward of a learned vector field that is trained with conditional flow matching. Sampling then proceeds by solving the differential equation given by the vector field. An advantage of this method over diffusion models is reduced training and sampling time. Flow matching has seen success in backbone generation [73, 115] and sampling protein ensembles [116].

Regardless of the exact shape of the field in the coming years, it is undeniable that diffusion models and similar frameworks will continue to be used in the design and prediction of biomolecules. They have introduced scalable, generative modeling to the field and have already demonstrated their advantages over previous traditional and machine-learning approaches by setting new state-of-the-art results in numerous problems.

6 Acknowledgments

This work was partially supported by the National Institute of General Medical Sciences [R35GM138146 to D.B.] and the National Science Foundation [DBI2208679 to D.B.].

References

- [1] Ian Goodfellow, Jean Pouget-Abadie, Mehdi Mirza, Bing Xu, David Warde-Farley, Sherjil Ozair, Aaron Courville, and Yoshua Bengio. Generative adversarial networks. *Communications of the ACM*, 63(11):139–144, 2020.
- [2] Prafulla Dhariwal and Alex Nichol. Diffusion models beat GANs on image synthesis, June 2021. arXiv:2105.05233 [cs, stat].
- [3] Florinel-Alin Croitoru, Vlad Hondru, Radu Tudor Ionescu, and Mubarak Shah. Diffusion models in vision: A survey. *IEEE Transactions on Pattern Analysis and Machine Intelligence*, 2023.
- [4] Vadim Popov, Ivan Vovk, Vladimir Gogoryan, Tasnima Sadekova, Mikhail Kudinov, and Jiansheng Wei. Diffusion-based voice conversion with fast maximum likelihood sampling scheme. *arXiv preprint arXiv:2109.13821*, 2021.
- [5] Shoule Wu and Ziqiang Shi. ItôTTS and ItôWave: Linear stochastic differential equation is all you need for audio generation. *arXiv preprint arXiv:2105.07583*, 2021.

- [6] Jinglin Liu, Chengxi Li, Yi Ren, Feiyang Chen, and Zhou Zhao. Diffsinger: Singing voice synthesis via shallow diffusion mechanism. In *Proceedings of the AAAI conference on artificial intelligence*, volume 36, pages 11020–11028, 2022.
- [7] Joao Carvalho, Mark Baierl, Julen Urain, and Jan Peters. Conditioned score-based models for learning collision-free trajectory generation. In *NeurIPS 2022 Workshop on Score-Based Methods*, 2022.
- [8] Joao Carvalho, An T Le, Mark Baierl, Dorothea Koert, and Jan Peters. Motion planning diffusion: Learning and planning of robot motions with diffusion models. In *2023 IEEE/RSJ International Conference on Intelligent Robots and Systems (IROS)*, pages 1916–1923. IEEE, 2023.
- [9] Ivan Kapelyukh, Vitalis Vosylius, and Edward Johns. Dall-e-bot: Introducing web-scale diffusion models to robotics. *IEEE Robotics and Automation Letters*, 2023.
- [10] Julen Urain, Niklas Funk, Jan Peters, and Georgia Chalvatzaki. SE (3)-diffusionfields: Learning smooth cost functions for joint grasp and motion optimization through diffusion. In *2023 IEEE International Conference on Robotics and Automation (ICRA)*, pages 5923–5930. IEEE, 2023.
- [11] Edmund Findlay, Haozheng Zhang, Ziyi Chang, and Hubert PH Shum. Denoising diffusion probabilistic models for styled walking synthesis. 2022.
- [12] Sidhartha Chaudhury, Sergey Lyskov, and Jeffrey J Gray. PyRosetta: a script-based interface for implementing molecular modeling algorithms using rosetta. *Bioinformatics*, 26(5):689–691, 2010.
- [13] David Ryan Koes, Matthew P Baumgartner, and Carlos J Camacho. Lessons learned in empirical scoring with smina from the CSAR 2011 benchmarking exercise. *Journal of chemical information and modeling*, 53(8):1893–1904, 2013.
- [14] Richard A Friesner, Jay L Banks, Robert B Murphy, Thomas A Halgren, Jasna J Klicic, Daniel T Mainz, Matthew P Repasky, Eric H Knoll, Mee Shelley, Jason K Perry, et al. Glide: a new approach for rapid, accurate docking and scoring. 1. method and assessment of docking accuracy. *Journal of medicinal chemistry*, 47(7):1739–1749, 2004.
- [15] Nana Heilmann, Moritz Wolf, Mariana Kozłowska, Elaheh Sedghamiz, Julia Setzler, Martin Brieg, and Wolfgang Wenzel. Sampling of the conformational landscape of small proteins with monte carlo methods. *Scientific reports*, 10(1):18211, 2020.
- [16] Cyrus Levinthal. How to fold graciously. *Mossbauer spectroscopy in biological systems*, 67:22–24, 1969.
- [17] John Jumper, Richard Evans, Alexander Pritzel, Tim Green, Michael Figurnov, Olaf Ronneberger, Kathryn Tunyasuvunakool, Russ Bates, Augustin Žídek, and Anna Potapenko. Highly accurate protein structure prediction with AlphaFold. *Nature*, 596(7873):583–589, 2021. Publisher: Nature Publishing Group.
- [18] Jianfeng Lu, Zuowei Shen, Haizhao Yang, and Shijun Zhang. Deep network approximation for smooth functions. *SIAM Journal on Mathematical Analysis*, 53(5):5465–5506, 2021.
- [19] Radford M Neal. Annealed importance sampling. *Statistics and computing*, 11:125–139, 2001.
- [20] Christopher Jarzynski. Equilibrium free-energy differences from nonequilibrium measurements: A master-equation approach. *Physical Review E*, 56(5):5018, 1997.
- [21] Jascha Sohl-Dickstein, Eric Weiss, Niru Maheswaranathan, and Surya Ganguli. Deep unsupervised learning using nonequilibrium thermodynamics. In *Proceedings of the 32nd International Conference on Machine Learning*, pages 2256–2265. PMLR, June 2015. ISSN: 1938-7228.
- [22] Jonathan Ho, Ajay Jain, and Pieter Abbeel. Denoising diffusion probabilistic models. In *Advances in Neural Information Processing Systems*, volume 33, pages 6840–6851. Curran Associates, Inc., 2020.

- [23] Yang Song and Stefano Ermon. Generative modeling by estimating gradients of the data distribution. In *Advances in Neural Information Processing Systems*, volume 32. Curran Associates, Inc., 2019.
- [24] Yang Song, Jascha Sohl-Dickstein, Diederik P. Kingma, Abhishek Kumar, Stefano Ermon, and Ben Poole. Score-based generative modeling through stochastic differential equations, November 2020.
- [25] Yang Song, Sahaj Garg, Jiaxin Shi, and Stefano Ermon. Sliced score matching: A scalable approach to density and score estimation. In *Uncertainty in Artificial Intelligence*, pages 574–584. PMLR, 2020.
- [26] Minkai Xu, Lantao Yu, Yang Song, Chence Shi, Stefano Ermon, and Jian Tang. Geodiff: A geometric diffusion model for molecular conformation generation. *arXiv preprint arXiv:2203.02923*, 2022.
- [27] Chence Shi, Shitong Luo, Minkai Xu, and Jian Tang. Learning gradient fields for molecular conformation generation. In *International conference on machine learning*, pages 9558–9568. PMLR, 2021.
- [28] Valentin De Bortoli, Emile Mathieu, Michael Hutchinson, James Thornton, Yee Whye Teh, and Arnaud Doucet. Riemannian score-based generative modelling, November 2022. arXiv:2202.02763 [cs, math, stat].
- [29] Bowen Jing, Gabriele Corso, Jeffrey Chang, Regina Barzilay, and Tommi Jaakkola. Torsional diffusion for molecular conformer generation, February 2023. arXiv:2206.01729 [physics, q-bio].
- [30] Chin-Wei Huang, Milad Aghajohari, Joey Bose, Prakash Panangaden, and Aaron C Courville. Riemannian diffusion models. *Advances in Neural Information Processing Systems*, 35:2750–2761, 2022.
- [31] Namrata Anand and Tudor Achim. Protein structure and sequence generation with equivariant denoising diffusion probabilistic models, May 2022. arXiv:2205.15019 [cs, q-bio].
- [32] Brian L. Trippe, Jason Yim, Doug Tischer, David Baker, Tamara Broderick, Regina Barzilay, and Tommi Jaakkola. Diffusion probabilistic modeling of protein backbones in 3D for the motif-scaffolding problem, March 2023. arXiv:2206.04119 [cs, q-bio, stat].
- [33] Gabriele Corso, Hannes Stärk, Bowen Jing, Regina Barzilay, and Tommi Jaakkola. DiffDock: Diffusion steps, twists, and turns for molecular docking, February 2023. arXiv:2210.01776 [physics, q-bio] version: 2.
- [34] Zhuoran Qiao, Weili Nie, Arash Vahdat, Thomas F. Miller III, and Anima Anandkumar. State-specific protein-ligand complex structure prediction with a multi-scale deep generative model, April 2023. arXiv:2209.15171 [cs, q-bio].
- [35] Joseph L. Watson, David Juergens, Nathaniel R. Bennett, Brian L. Trippe, Jason Yim, Helen E. Eisenach, Woody Ahern, Andrew J. Borst, Robert J. Ragotte, Lukas F. Milles, Basile I. M. Wicky, Nikita Hanikel, Samuel J. Pellock, Alexis Courbet, William Sheffler, Jue Wang, Preetham Venkatesh, Isaac Sappington, Susana Vázquez Torres, Anna Lauko, Valentin De Bortoli, Emile Mathieu, Sergey Ovchinnikov, Regina Barzilay, Tommi S. Jaakkola, Frank DiMaio, Minkyung Baek, and David Baker. De novo design of protein structure and function with RFdiffusion. *Nature*, 620(7976):1089–1100, August 2023. Number: 7976 Publisher: Nature Publishing Group.
- [36] Josh Abramson, Jonas Adler, Jack Dunger, Richard Evans, Tim Green, Alexander Pritzel, Olaf Ronneberger, Lindsay Willmore, Andrew J Ballard, Joshua Bambrick, et al. Accurate structure prediction of biomolecular interactions with AlphaFold 3. *Nature*, pages 1–3, 2024.
- [37] Nathaniel Thomas, Tess Smidt, Steven Kearnes, Lusann Yang, Li Li, Kai Kohlhoff, and Patrick Riley. Tensor field networks: Rotation-and translation-equivariant neural networks for 3d point clouds. *arXiv preprint arXiv:1802.08219*, 2018.
- [38] Victor Garcia Satorras, Emiel Hoogeboom, and Max Welling. E(n) Equivariant Graph Neural Networks. In *Proceedings of the 38th International Conference on Machine Learning*, pages 9323–9332. PMLR, July 2021. ISSN: 2640-3498.

- [39] Dmitry I. Nikolayev and Tatjana I. Savyolov. Normal distribution on the rotation group $SO(3)$. *Texture, Stress, and Microstructure*, 29:201–233, 1997. Publisher: Hindawi.
- [40] Diederik P. Kingma and Prafulla Dhariwal. Glow: Generative flow with invertible 1x1 convolutions, July 2018. arXiv:1807.03039 [cs, stat].
- [41] John B. Ingraham, Max Baranov, Zak Costello, Karl W. Barber, Wujie Wang, Ahmed Ismail, Vincent Frappier, Dana M. Lord, Christopher Ng-Thow-Hing, Erik R. Van Vlack, Shan Tie, Vincent Xue, Sarah C. Cowles, Alan Leung, João V. Rodrigues, Claudio L. Morales-Perez, Alex M. Ayoub, Robin Green, Katherine Puentes, Frank Oplinger, Nishant V. Panwar, Fritz Obermeyer, Adam R. Root, Andrew L. Beam, Frank J. Poelwijk, and Gevorg Grigoryan. Illuminating protein space with a programmable generative model. *Nature*, 623(7989):1070–1078, November 2023. Publisher: Nature Publishing Group.
- [42] Rohith Krishna, Jue Wang, Woody Ahern, Pascal Sturmfels, Preetham Venkatesh, Indrek Kalvet, Gyu Rie Lee, Felix S Morey-Burrows, Ivan Anishchenko, Ian R Humphreys, et al. Generalized biomolecular modeling and design with RoseTTAFold all-atom. *Science*, 384(6693):ead12528, 2024.
- [43] Yeqing Lin and Mohammed AlQuraishi. Generating novel, designable, and diverse protein structures by equivariantly diffusing oriented residue clouds, June 2023. arXiv:2301.12485 [cs, q-bio].
- [44] Kevin E. Wu, Kevin K. Yang, Rianne van den Berg, Sarah Alamdari, James Y. Zou, Alex X. Lu, and Ava P. Amini. Protein structure generation via folding diffusion. *Nature Communications*, 15(1):1059, February 2024. Publisher: Nature Publishing Group.
- [45] Jin Sub Lee, Jisun Kim, and Philip M. Kim. Score-based generative modeling for de novo protein design. *Nature Computational Science*, 3(5):382–392, May 2023. Number: 5 Publisher: Nature Publishing Group.
- [46] Jason Yim, Brian L. Trippe, Valentin De Bortoli, Emile Mathieu, Arnaud Doucet, Regina Barzilay, and Tommi Jaakkola. SE(3) diffusion model with application to protein backbone generation, May 2023. arXiv:2302.02277 [cs, q-bio, stat].
- [47] Cong Fu, Keqiang Yan, Limei Wang, Wing Yee Au, Michael McThrow, Tao Komikado, Koji Maruhashi, Kanji Uchino, Xiaoning Qian, and Shuiwang Ji. A latent diffusion model for protein structure generation, May 2023. arXiv:2305.04120 [cs, q-bio].
- [48] Cheng Zhang, Adam Leach, Thomas Makkink, Miguel Arbesú, Ibtissem Kadri, Daniel Luo, Liron Mizrahi, Sabrine Krichen, Maren Lang, Andrey Tovchigrechko, Nicolas Lopez Carranza, Uğur Şahin, Karim Beguir, Michael Rooney, and Yunguan Fu. FrameDiPT: SE(3) diffusion model for protein structure inpainting, January 2024. Pages: 2023.11.21.568057 Section: New Results.
- [49] Jiarui Lu, Bozita Zhong, Zuobai Zhang, and Jian Tang. Str2Str: A score-based framework for zero-shot protein conformation sampling. October 2023.
- [50] Shuxin Zheng, Jiyan He, Chang Liu, Yu Shi, Ziheng Lu, Weitao Feng, Fusong Ju, Jiayi Wang, Jianwei Zhu, Yaosen Min, et al. Predicting equilibrium distributions for molecular systems with deep learning. *Nature Machine Intelligence*, pages 1–10, 2024.
- [51] Marloes Arts, Victor Garcia Satorras, Chin-Wei Huang, Daniel Zügner, Marco Federici, Cecilia Clementi, Frank Noé, Robert Pinsler, and Rianne van den Berg. Two for one: Diffusion models and force fields for coarse-grained molecular dynamics. *Journal of Chemical Theory and Computation*, 19(18):6151–6159, 2023.
- [52] Alexander E. Chu, Lucy Cheng, Gina El Nesr, Minkai Xu, and Po-Ssu Huang. An all-atom protein generative model, May 2023. Pages: 2023.05.24.542194 Section: New Results.
- [53] Alex Morehead, Jeffrey Ruffolo, Aadyot Bhatnagar, and Ali Madani. Towards joint sequence-structure generation of nucleic acid and protein complexes with SE(3)-discrete diffusion, December 2023. arXiv:2401.06151 [cs, q-bio].

- [54] Zehui Li, Yuhao Ni, Tim August B. Huygelen, Akashaditya Das, Guoxuan Xia, Guy-Bart Stan, and Yiren Zhao. Latent diffusion model for DNA sequence generation, December 2023. arXiv:2310.06150 [cs].
- [55] Sarah Alamdari, Nitya Thakkar, Rianne van den Berg, Alex X. Lu, Nicolo Fusi, Ava P. Amini, and Kevin K. Yang. Protein generation with evolutionary diffusion: sequence is all you need, September 2023. Pages: 2023.09.11.556673 Section: New Results.
- [56] Sidney Lyayuga Lisanza, Jake Merle Gershon, Sam Tipps, Lucas Arnoldt, Samuel Hendel, Jeremiah Nelson Sims, Xinting Li, and David Baker. Joint generation of protein sequence and structure with RoseTTAFold sequence space diffusion, May 2023. Pages: 2023.05.08.539766 Section: New Results.
- [57] Bo Ni, David L. Kaplan, and Markus J. Buehler. ForceGen: End-to-end de novo protein generation based on nonlinear mechanical unfolding responses using a protein language diffusion model, October 2023. arXiv:2310.10605 [cond-mat, q-bio].
- [58] Bingxin Zhou, Lirong Zheng, Banghao Wu, Kai Yi, Bozitao Zhong, Pietro Liò, and Liang Hong. Conditional protein denoising diffusion generates programmable endonucleases, August 2023. Pages: 2023.08.10.552783 Section: New Results.
- [59] Gabriele Corso, Arthur Deng, Benjamin Fry, Nicholas Polizzi, Regina Barzilay, and Tommi Jaakkola. Deep confident steps to new pockets: Strategies for docking generalization. *arXiv preprint arXiv:2402.18396*, 2024.
- [60] Matthew R Masters, Amr H Mahmoud, and Markus A Lill. Fusiondock: physics-informed diffusion model for molecular docking. In *ICML workshop on Computational Biology*, 2023.
- [61] Shuya Nakata, Yoshiharu Mori, and Shigenori Tanaka. End-to-end protein–ligand complex structure generation with diffusion-based generative models. *BMC Bioinformatics*, 24(1):233, June 2023.
- [62] Michael S Jones, Kirill Shmilovich, and Andrew L Ferguson. DiAMoNDBack: Diffusion-denoising autoregressive model for non-deterministic backmapping of α protein traces. *Journal of Chemical Theory and Computation*, 19(21):7908–7923, 2023.
- [63] Yikai Liu, Guang Lin, and Ming Chen. Backdiff: a diffusion model for generalized transferable protein backmapping. 2023.
- [64] Mohamed Amine Ketata, Cedrik Laue, Ruslan Mammadov, Hannes Stärk, Menghua Wu, Gabriele Corso, Céline Marquet, Regina Barzilay, and Tommi S. Jaakkola. DiffDock-PP: Rigid protein-protein docking with diffusion models, April 2023. arXiv:2304.03889 [cs, q-bio].
- [65] Yangtian Zhang, Zuobai Zhang, Bozitao Zhong, Sanchit Misra, and Jian Tang. DiffPack: A torsional diffusion model for autoregressive protein side-chain packing, June 2023. arXiv:2306.01794 [cs, q-bio].
- [66] Runze Zhang, Xinyu Jiang, Duanhua Cao, Jie Yu, Mingan Chen, Zhehuan Fan, Xiangtai Kong, Jiacheng Xiong, Zimei Zhang, Wei Zhang, et al. PackDock: a diffusion based side chain packing model for flexible protein-ligand docking. *bioRxiv*, pages 2024–01, 2024.
- [67] Bowen Jing, Ezra Erives, Peter Pao-Huang, Gabriele Corso, Bonnie Berger, and Tommi Jaakkola. EigenFold: Generative protein structure prediction with diffusion models, April 2023. arXiv:2304.02198 [physics, q-bio].
- [68] Kai Yi, Bingxin Zhou, Yiqing Shen, Pietro Lió, and Yuguang Wang. Graph denoising diffusion for inverse protein folding. *Advances in Neural Information Processing Systems*, 36:10238–10257, December 2023.
- [69] Zeming Lin, Halil Akin, Roshan Rao, Brian Hie, Zhongkai Zhu, Wenting Lu, Nikita Smetanin, Robert Verkuil, Ori Kabeli, Yaniv Shmueli, et al. Evolutionary-scale prediction of atomic-level protein structure with a language model. *Science*, 379(6637):1123–1130, 2023.

- [70] Justas Dauparas, Ivan Anishchenko, Nathaniel Bennett, Hua Bai, Robert J Ragotte, Lukas F Milles, Basile IM Wicky, Alexis Courbet, Rob J de Haas, Neville Bethel, et al. Robust deep learning–based protein sequence design using ProteinMPNN. *Science*, 378(6615):49–56, 2022.
- [71] Jianyi Yang, Ivan Anishchenko, Hahnbeom Park, Zhenling Peng, Sergey Ovchinnikov, and David Baker. Improved protein structure prediction using predicted interresidue orientations. *Proceedings of the National Academy of Sciences*, 117(3):1496–1503, 2020.
- [72] Minkyung Baek, Frank DiMaio, Ivan Anishchenko, Justas Dauparas, Sergey Ovchinnikov, Gyu Rie Lee, Jue Wang, Qian Cong, Lisa N Kinch, R Dustin Schaeffer, et al. Accurate prediction of protein structures and interactions using a three-track neural network. *Science*, 373(6557):871–876, 2021.
- [73] Avishek Joey Bose, Tara Akhound-Sadegh, Kilian Fatras, Guillaume Huguet, Jarrod Rector-Brooks, Cheng-Hao Liu, Andrei Cristian Nica, Maksym Korablyov, Michael Bronstein, and Alexander Tong. SE (3)-stochastic flow matching for protein backbone generation. *arXiv preprint arXiv:2310.02391*, 2023.
- [74] Jacob Austin, Daniel D. Johnson, Jonathan Ho, Daniel Tarlow, and Rianne van den Berg. Structured denoising diffusion models in discrete state-spaces, February 2023. arXiv:2107.03006 [cs].
- [75] Ahmed Elnaggar, Michael Heinzinger, Christian Dallago, Ghalia Rehawi, Yu Wang, Llion Jones, Tom Gibbs, Tamas Feher, Christoph Angerer, Martin Steinegger, Debsindhu Bhowmik, and Burkhard Rost. ProtTrans: Toward understanding the language of life through self-supervised learning. *IEEE Transactions on Pattern Analysis and Machine Intelligence*, 44(10):7112–7127, October 2022. Conference Name: IEEE Transactions on Pattern Analysis and Machine Intelligence.
- [76] Robert Verkuil, Ori Kabeli, Yilun Du, Basile I. M. Wicky, Lukas F. Milles, Justas Dauparas, David Baker, Sergey Ovchinnikov, Tom Sercu, and Alexander Rives. Language models generalize beyond natural proteins, December 2022. Pages: 2022.12.21.521521 Section: New Results.
- [77] Ruidong Wu, Fan Ding, Rui Wang, Rui Shen, Xiwen Zhang, Shitong Luo, Chenpeng Su, Zuofan Wu, Qi Xie, Bonnie Berger, et al. High-resolution de novo structure prediction from primary sequence. *BioRxiv*, pages 2022–07, 2022.
- [78] Bingxin Zhou, Lirong Zheng, Banghao Wu, Kai Yi, Bozitao Zhong, Pietro Lio, and Liang Hong. Conditional protein denoising diffusion generates programmable endonucleases. *bioRxiv*, pages 2023–08, 2023.
- [79] Robin Rombach, Andreas Blattmann, Dominik Lorenz, Patrick Esser, and Björn Ommer. High-resolution image synthesis with latent diffusion models. In *Proceedings of the IEEE/CVF conference on computer vision and pattern recognition*, pages 10684–10695, 2022.
- [80] Michael Feig and Vahid Mirjalili. Protein structure refinement via molecular-dynamics simulations: what works and what does not? *Proteins: Structure, Function, and Bioinformatics*, 84:282–292, 2016.
- [81] Michael Feig. Computational protein structure refinement: almost there, yet still so far to go. *Wiley Interdisciplinary Reviews: Computational Molecular Science*, 7(3):e1307, 2017.
- [82] Lim Heo and Michael Feig. Prefmd: a web server for protein structure refinement via molecular dynamics simulations. *Bioinformatics*, 34(6):1063–1065, 2018.
- [83] Lim Heo and Michael Feig. Experimental accuracy in protein structure refinement via molecular dynamics simulations. *Proceedings of the National Academy of Sciences*, 115(52):13276–13281, 2018.
- [84] Vahid Mirjalili and Michael Feig. Protein structure refinement through structure selection and averaging from molecular dynamics ensembles. *Journal of chemical theory and computation*, 9(2):1294–1303, 2013.

- [85] Vahid Mirjalili, Keenan Noyes, and Michael Feig. Physics-based protein structure refinement through multiple molecular dynamics trajectories and structure averaging. *Proteins: Structure, Function, and Bioinformatics*, 82:196–207, 2014.
- [86] Kresten Lindorff-Larsen, Stefano Piana, Ron O Dror, and David E Shaw. How fast-folding proteins fold. *Science*, 334(6055):517–520, 2011.
- [87] Fang Wu and Stan Z. Li. DiffMD: A geometric diffusion model for molecular dynamics simulations. *Proceedings of the AAAI Conference on Artificial Intelligence*, 37(4):5321–5329, June 2023. Number: 4.
- [88] Tim Hsu, Babak Sadigh, Vasily Bulatov, and Fei Zhou. Score dynamics: scaling molecular dynamics with picosecond timesteps via conditional diffusion model, October 2023. arXiv:2310.01678 [physics].
- [89] Jonas Köhler, Yaoyi Chen, Andreas Krämer, Cecilia Clementi, and Frank Noé. Flow-matching – efficient coarse-graining of molecular dynamics without forces. *Journal of Chemical Theory and Computation*, 19(3):942–952, February 2023. arXiv:2203.11167 [physics].
- [90] Xiaoqiang Huang, Robin Pearce, and Yang Zhang. FASPR: an open-source tool for fast and accurate protein side-chain packing. *Bioinformatics*, 36(12):3758–3765, 2020.
- [91] Chen Yanover, Ora Schueler-Furman, and Yair Weiss. Minimizing and learning energy functions for side-chain prediction. *Journal of Computational Biology*, 15(7):899–911, 2008.
- [92] Shide Liang, Dandan Zheng, Chi Zhang, and Daron M Standley. Fast and accurate prediction of protein side-chain conformations. *Bioinformatics*, 27(20):2913–2914, 2011.
- [93] Aleksandra E Badaczewska-Dawid, Andrzej Kolinski, and Sebastian Kmiecik. Computational reconstruction of atomistic protein structures from coarse-grained models. *Computational and structural biotechnology journal*, 18:162–176, 2020.
- [94] Rebecca F Alford, Andrew Leaver-Fay, Jeliasko R Jeliaskov, Matthew J O’Meara, Frank P DiMaio, Hahnbeom Park, Maxim V Shapovalov, P Douglas Renfrew, Vikram K Mulligan, Kalli Kappel, et al. The Rosetta all-atom energy function for macromolecular modeling and design. *Journal of chemical theory and computation*, 13(6):3031–3048, 2017.
- [95] Georgii G Krivov, Maxim V Shapovalov, and Roland L Dunbrack Jr. Improved prediction of protein side-chain conformations with SCWRL4. *Proteins: Structure, Function, and Bioinformatics*, 77(4):778–795, 2009.
- [96] Jinbo Xu and Bonnie Berger. Fast and accurate algorithms for protein side-chain packing. *Journal of the ACM (JACM)*, 53(4):533–557, 2006.
- [97] Yang Cao, Lin Song, Zhichao Miao, Yun Hu, Liqing Tian, and Taijiao Jiang. Improved side-chain modeling by coupling clash-detection guided iterative search with rotamer relaxation. *Bioinformatics*, 27(6):785–790, 2011.
- [98] Matt McPartlon and Jinbo Xu. An end-to-end deep learning method for rotamer-free protein side-chain packing. *bioRxiv*, pages 2022–03, 2022. Publisher: Cold Spring Harbor Laboratory.
- [99] Mikita Misiura, Raghav Shroff, Ross Thyer, and Anatoly B Kolomeisky. DLPacker: Deep learning for prediction of amino acid side chain conformations in proteins. *Proteins: Structure, Function, and Bioinformatics*, 90(6):1278–1290, 2022.
- [100] Oleg Trott and Arthur J Olson. AutoDock Vina: improving the speed and accuracy of docking with a new scoring function, efficient optimization, and multithreading. *Journal of computational chemistry*, 31(2):455–461, 2010.

- [101] Richard Evans, Michael O’Neill, Alexander Pritzel, Natasha Antropova, Andrew Senior, Tim Green, Augustin Židek, Russ Bates, Sam Blackwell, Jason Yim, et al. Protein complex prediction with AlphaFold-Multimer. *bioRxiv*, pages 2021–10, 2021.
- [102] Diederik P Kingma and Max Welling. Auto-encoding variational bayes. *arXiv preprint arXiv:1312.6114*, 2013.
- [103] Steven Henikoff and Jorja G Henikoff. Amino acid substitution matrices from protein blocks. *Proceedings of the National Academy of Sciences*, 89(22):10915–10919, 1992.
- [104] René Thomsen and Mikael H Christensen. MolDock: a new technique for high-accuracy molecular docking. *Journal of medicinal chemistry*, 49(11):3315–3321, 2006.
- [105] Hannes Stärk, Octavian Ganea, Lagnajit Pattanaik, Regina Barzilay, and Tommi Jaakkola. Equibind: Geometric deep learning for drug binding structure prediction. In *International conference on machine learning*, pages 20503–20521. PMLR, 2022.
- [106] Wei Lu, Qifeng Wu, Jixian Zhang, Jiahua Rao, Chengtao Li, and Shuangjia Zheng. Tankbind: Trigonometry-aware neural networks for drug-protein binding structure prediction. *Advances in neural information processing systems*, 35:7236–7249, 2022.
- [107] Zhihai Liu, Minyi Su, Li Han, Jie Liu, Qifan Yang, Yan Li, and Renxiao Wang. Forging the basis for developing protein–ligand interaction scoring functions. *Accounts of chemical research*, 50(2):302–309, 2017.
- [108] Yuejiang Yu, Shuqi Lu, Zhifeng Gao, Hang Zheng, and Guolin Ke. Do deep learning models really outperform traditional approaches in molecular docking? *arXiv preprint arXiv:2302.07134*, 2023.
- [109] Ganesh Chandan Kanakala, Rishal Aggarwal, Divya Nayar, and U Deva Priyakumar. Latent biases in machine learning models for predicting binding affinities using popular data sets. *ACS omega*, 8(2):2389–2397, 2023.
- [110] Jie Li, Xingyi Guan, Oufan Zhang, Kunyang Sun, Yingze Wang, Dorian Bagni, and Teresa Head-Gordon. Leak proof PDBBind: A reorganized dataset of protein-ligand complexes for more generalizable binding affinity prediction. *ArXiv*, 2023.
- [111] Martin Butterschoen, Garrett M Morris, and Charlotte M Deane. PoseBusters: AI-based docking methods fail to generate physically valid poses or generalise to novel sequences. *Chemical Science*, 2024.
- [112] Alex Graves, Rupesh Kumar Srivastava, Timothy Atkinson, and Faustino Gomez. Bayesian flow networks. *arXiv preprint arXiv:2308.07037*, 2023.
- [113] Yuxuan Song, Jingjing Gong, Hao Zhou, Mingyue Zheng, Jingjing Liu, and Wei-Ying Ma. Unified generative modeling of 3d molecules with bayesian flow networks. In *The Twelfth International Conference on Learning Representations*, 2023.
- [114] Yaron Lipman, Ricky TQ Chen, Heli Ben-Hamu, Maximilian Nickel, and Matt Le. Flow matching for generative modeling. *arXiv preprint arXiv:2210.02747*, 2022.
- [115] Jason Yim, Andrew Campbell, Andrew YK Foong, Michael Gastegger, José Jiménez-Luna, Sarah Lewis, Victor Garcia Satorras, Bastiaan S Veeling, Regina Barzilay, Tommi Jaakkola, et al. Fast protein backbone generation with SE (3) flow matching. *arXiv preprint arXiv:2310.05297*, 2023.
- [116] Bowen Jing, Bonnie Berger, and Tommi Jaakkola. AlphaFold meets flow matching for generating protein ensembles. *arXiv preprint arXiv:2402.04845*, 2024.
- [117] Yang Zhang and Jeffrey Skolnick. TM-align: a protein structure alignment algorithm based on the tm-score. *Nucleic acids research*, 33(7):2302–2309, 2005.

- [118] Michel van Kempen, Stephanie S Kim, Charlotte Tumescheit, Milot Mirdita, Cameron LM Gilchrist, Johannes Söding, and Martin Steinegger. Foldseek: fast and accurate protein structure search. *Biorxiv*, pages 2022–02, 2022.
- [119] Helen Berman, Kim Henrick, and Haruki Nakamura. Announcing the worldwide protein data bank. *Nature structural & molecular biology*, 10(12):980–980, 2003.
- [120] Sheng Wang, Jian Peng, Jianzhu Ma, and Jinbo Xu. Protein secondary structure prediction using deep convolutional neural fields. *Scientific reports*, 6(1):1–11, 2016.
- [121] Christine A Orengo, Alex D Michie, Susan Jones, David T Jones, Mark B Swindells, and Janet M Thornton. Cath—a hierarchic classification of protein domain structures. *Structure*, 5(8):1093–1109, 1997.
- [122] John Ingraham, Vikas Garg, Regina Barzilay, and Tommi Jaakkola. Generative models for graph-based protein design. *Advances in neural information processing systems*, 32, 2019.
- [123] Bowen Jing, Stephan Eismann, Patricia Suriana, Raphael John Lamarre Townshend, and Ron Dror. Learning from protein structure with geometric vector perceptrons. In *International Conference on Learning Representations*, 2020.
- [124] Cheng Tan, Zhangyang Gao, Jun Xia, Bozhen Hu, and Stan Z Li. Generative de novo protein design with global context. *arXiv preprint arXiv:2204.10673*, 2022.
- [125] Chloe Hsu, Robert Verkuil, Jason Liu, Zeming Lin, Brian Hie, Tom Sercu, Adam Lerer, and Alexander Rives. Learning inverse folding from millions of predicted structures. In *International conference on machine learning*, pages 8946–8970. PMLR, 2022.
- [126] Zhangyang Gao, Cheng Tan, and Stan Z Li. Alphadesign: A graph protein design method and benchmark on alphafolddb. *arXiv preprint arXiv:2202.01079*, 2022.
- [127] Zhangyang Gao, Cheng Tan, Pablo Chacón, and Stan Z Li. PiFold: Toward effective and efficient protein inverse folding. *arXiv preprint arXiv:2209.12643*, 2022.
- [128] Hua Cheng, R Dustin Schaeffer, Yuxing Liao, Lisa N Kinch, Jimin Pei, Shuoyong Shi, Bong-Hyun Kim, and Nick V Grishin. ECOD: an evolutionary classification of protein domains. *PLoS computational biology*, 10(12):e1003926, 2014.
- [129] Andrew T McNutt, Paul Francoeur, Rishal Aggarwal, Tomohide Masuda, Rocco Meli, Matthew Ragoza, Jocelyn Sunseri, and David Ryan Koes. GNINA 1.0: molecular docking with deep learning. *Journal of cheminformatics*, 13(1):43, 2021.
- [130] Radoslav Krivák and David Hoksza. P2Rank: machine learning based tool for rapid and accurate prediction of ligand binding sites from protein structure. *Journal of cheminformatics*, 10:1–12, 2018.

A Benchmarking details

A.1 Backbone generation methods

We focus on methods that were able to generate proteins up to 250 amino acids long. We generated 50 proteins each for lengths 50, 100, 150, 200, and 250 (giving a total of 250 generated samples). To test designability, we used ProteinMPNN [70] at a temperature of 0.1 to create 8 possible sequences, which were then folded using ESMFold [69]. The minimum difference between the RMSD of the folded C α backbones and the corresponding sample was recorded as the scRMSD for the structure. A protein is considered designable if scRMSD is less than 2.0 Å, and the percentage of designable proteins is reported for each method. To measure diversity, TM-align [117] is used to compare each pair of designable proteins from a method (normalizing with the length of the longer protein). The average TM-Score is recorded for each method. To measure novelty, we used FoldSeek [118] to compare the designable proteins against the PDB

[119]. The TM-Score is computed against proteins in the PDB and the maximum is recorded as PDBTM. If PDBTM is less than 0.5, then the generated structure is considered novel. The percentage of novel proteins is recorded.

A.2 DiffPack

Training and validation used BC40 [120] and followed the dataset split given in AttnPacker [98]. The models were then evaluated on CASP13 and CASP14 datasets. The training set was curated to remove sequences with 40% or more similarity to those in the test set. Both deep learning methods, like AttnPacker [98] and DLPacker [99], and traditional methods, like SCWRL4 [95], FASPR [90], and RosettaPacker [12], are used as baselines for DiffPack.

For each model the angle MAE, angle accuracy, and atom RMSD are computed. Angle MAE is the mean absolute error of the predicted side-chain torsional angles versus the actual angles. Angle accuracy is the percentage of angles that are within 20deg of the actual angle. Atom RMSD is the average RMSD of the side-chain atoms for each residue. Results are further categorized by “Core” and “Surface” residues. Residues are labeled as core residues if at least 20 C_β atoms are within a 10 Å radius. Surface residues have at most 15 C_β atoms within the same radius.

A.3 Eigenfold

The test set in the Eigenfold paper [67] is CAMEO targets released between August 1st, 2022 and October 31st, 2022 with lengths of less than 750 residues. The Eigenfold method was benchmarked against other structure prediction methods: namely, AlphaFold2 [17], ESMFold [69], OmegaFold [77], and RoseTTAFold [72]. For each method, five protein structures were generated and ranked based on an approximate ELBO. The top-ranked structure was taken as the final prediction and compared against the native structure. The metrics in table 4 are the results of these comparisons.

A.4 GraDe-IF

The inverse folding methods were tested on recovering protein sequences in CATH [121]. The training-validation-training split follows the CATH v4.2.0-based partitioning as done for GraphTrans [122] and GVP [123]. Testing was further split into three categories: short, single-chain, and all. *Short* refers to proteins of length less than 100 residues. *Single-chain* refers to proteins with only one chain. The methods were evaluated on *perplexity* and *recovery rate*. Perplexity measures how well the predicted amino acid probabilities match the actual amino acids at each position. A lower perplexity means that the model better fits the distribution of the data. The recovery rate measures the percentage of amino acids that are correctly predicted from the original sequences. A higher recovery rate indicates the model is better at predicting the original sequence. In addition, the training data set for each model is given in table 5: CATH version 4.2 or 4.3.

GraDe-IF was benchmarked against other inverse folding methods, including StructGNN [122], GraphTrans [122], GCA [124], GVP [123], GVP-large [125], AlphaDesign [126], ESM-if1 [125], ProteinMPNN [70], and PiFold [127].

A.5 DiffDock-L

The benchmarking in [59] was performed on the PDBBind dataset [107] and the authors’ new dataset, DockGen. The main aim of the dataset was to provide better benchmarks for the protein-ligand docking problem by preventing data leakage between training and testing data. For instance, proteins with less than 30% sequence similarity may nonetheless share very similar binding pockets, and so benchmarking must account for these structural similarities when doing a split of training and testing. The authors use the ECOD [128] classification to determine the protein domain of the chain making the most contacts with the ligand. This is used to cluster the complexes with an equal number of clusters being assigned to the training and testing datasets. Further filtering steps are taken (such as removing protein-ligand complexes with multiple ligands binding to the same pocket) to reach the final benchmark dataset.

The benchmarking was carried out on both search-based and ML methods. The search-based methods included SMINA [89] and GNINA [129]. Since search-based methods have improved blind docking results by first selecting a pocket with a pocket finder method, results when using P2Rank [130] prior to docking are also recorded. The ML methods include Equibind [105], TankBind [106], and DiffDock [33]. For the DiffDock models, the number of poses sampled is also provided by the number in parentheses.